

UNIVERSITY OF OKLAHOMA
GRADUATE COLLEGE

QUANTIFYING THE IMPACT OF ASPHALTENE PRECIPITATION ON
SANDSTONE WETTABILITY

A THESIS
SUBMITTED TO THE GRADUATE FACULTY
in partial fulfillment of the requirements for the
Degree of
MASTER OF SCIENCE

By
JOCIN JAMES ABRAHAM
Norman, Oklahoma
2017

QUANTIFYING THE IMPACT OF ASPHALTENE PRECIPITATION ON
SANDSTONE WETTABILITY

A THESIS APPROVED FOR THE
MEWBOURNE SCHOOL OF PETROLEUM AND GEOLOGICAL ENGINEERING

BY

Dr. Mashhad Fahes, Chair

Dr. Zulfiqar Reza

Dr. Catalin Teodoriu

Acknowledgements

I would like to sincerely express my thanks and appreciation to my committee chair, Dr. Mashhad Fahes, for her guidance, encouragement and support throughout my Master's program and the research behind this thesis. I would also like to express my gratitude to Dr. Zulfiqar Reza and Dr. Catalin Teodoriu for serving on my thesis committee and for their support and valued input.

I would also like to thank Gary Stowe and all my colleagues in the lab for their useful suggestions and for helping me out with the equipment's and experiments. Special thanks to Mohamed Mehana for the support and advise he provided during my research, and for going over the thesis. I am also grateful to my colleagues at University of Oklahoma and my friends who have supported me along the way.

Finally, I am highly indebted to my family for their endless support and patience. Thank you all for always being there for me. Boomer Sooner!

Jocin James Abraham

Class of 2017

Table of Contents

Acknowledgements	iv
Table of Contents	v
List of Tables	viii
List of Figures.....	ix
Abstract.....	xiii
CHAPTER 1: INTRODUCTION.....	1
1.1 What are Asphaltenes?	1
1.2 Causes of Asphaltene Precipitation and Factors Affecting the Deposition....	2
1.3 Deposition Mechanism.....	5
1.4 Problems Caused by Asphaltenes.....	8
1.5 Field Examples	10
1.5.1 Abu Dhabi	10
1.5.2 Rhourd-Nouss Sud Est Field, Algeria	11
1.5.3 Prinos Field.....	11
1.5.4 Hassi Massaoud Field, Algeria.....	12
1.5.5 Magwa Marrat Reservoir, Kuwait.....	12
1.6 Industry Methods to Mitigate Asphaltene Problems	13
CHAPTER 2: LITERATURE REVIEW	15
CHAPTER 3: CONCEPTS AND THEORETICAL BACKGROUND.....	25
3.1 Asphaltene Content Measurements	25
3.2 Porosity.....	26
3.3 Permeability.....	27

3.4	Wettability and Spontaneous Imbibition	31
3.5	Relative Permeability	33
CHAPTER 4: EXPERIMENTAL DESIGN AND METHODOLOGY.....		37
4.1	Objective.....	37
4.2	Experimental Workflow	37
4.3	Equipment and Materials.....	38
4.3.1	Rocks	38
4.3.2	Fluids and Gases.....	38
4.3.3	Equipment.....	40
4.4	Characterizing the Crude and Deposition Potential	40
4.4.1	Measuring Asphaltene Content	40
4.4.2	Deposition Potential	41
4.5	Rock Preparation	43
4.5.1	Porosity.....	43
4.5.2	Permeability.....	45
4.6	Uniformity of Deposition	48
4.6.1	Injection.....	48
4.6.2	Vacuum Saturation	50
4.6.3	Evaluating by Density, Permeability and Sample Sizes.....	53
4.6.4	Evaluating by TOC.....	55
4.7	Evaluating Wettability Alteration.....	56
4.7.1	Evaluating Pressure Drop Through Core flooding.....	56
4.7.2	Imbibition Tests.....	59

4.8	Relative Permeability Tests	61
4.9	CMG Modeling	64
CHAPTER 5: RESULTS AND DISCUSSION		67
5.1	Texas Crude and its Deposition Potential	67
5.2	Measuring Rock Properties	70
5.3	Uniformity of Deposition	73
5.4	Core Flood Pressure Drop Tests.....	79
5.5	Spontaneous Imbibition Tests	84
5.6	Relative Permeability Tests	89
5.7	CMG Modeling Results.....	94
CHAPTER 6: CONCLUSIONS AND RECOMMENDATIONS		99
6.1	Conclusions	99
6.2	Recommendations	101
References		102

List of Tables

Table 1: Fluids used in the experiments, and their properties (at 20°C)	39
Table 2: Rock and fluid properties specified in the CMG model.....	65
Table 3: Asphaltene content of Texas crude	67
Table 4: Physical properties of cores used in the study.....	70
Table 5: List of cores used for testing uniformity	74
Table 6: Permeability & density of the cores before and after exposure to crude	74
Table 7: Permeability and density of smaller cut samples	76
Table 8: Cores used for pressure drop tests.....	79
Table 9: Cores used for spontaneous imbibition, and the treatments done on them.	85
Table 10: Cores used for relative permeability tests.	89
Table 11: Relative permeability data points for Brine-Heptane flow.	90
Table 12: Brine-Heptane relative permeability endpoints for core exposed to crude	92

List of Figures

Figure 1: Asphaltene molecules, showing the stacked multi-ring structures (Akbarzadeh, et al., 2007)	1
Figure 2: Asphaltene deposition in pipes (Akbarzadeh, et al., 2007).....	2
Figure 3: Asphaltene precipitation behavior as shown by a sample phase envelope (Zendehboudi, et al., 2014).....	3
Figure 4: Asphaltene aggregation mechanism based on the Yen-Mullins model showing the clumping of asphaltene molecules (Vargas, et al., 2014).....	6
Figure 5: Asphaltene deposition and plugging mechanism (Kord, Mohammadzadeh, Miri, & Soulgani, 2013)	7
Figure 6: Asphaltene content of some crudes from around the world (Stankiewicz, 2009).....	10
Figure 7: Oil permeability reduction in Fontainebleau and Vosges sandstones following injection with crude (Minssieux, Nabzar, Chauveteau, Longeron, & Bensalem, 1998)	16
Figure 8: Relative permeability curves pre- and post-adsorption stages showing a shift in the endpoints (Hematfar, Maini, & Chen, 2013).....	21
Figure 9: Influence of asphaltene deposition on permeability of core samples for oils with different asphaltene contents (Shedid, 2001)	22
Figure 10: Influence of asphaltene deposition on relative permeability curves for cores created with different crudes (Shedid, 2001)	22
Figure 11: Influence of crudes with different asphaltene content on cumulative oil production and bottom-hole pressure of a reservoir (Nasri & Dabir, 2009)	23

Figure 12: An example calculation of permeability using Darcy equation shows deviation from linear trend in lab experiments. Higher flow region at the top right.	29
Figure 13: Calculation of permeability of our samples using Forchheimer equation for the non-Darcy region	30
Figure 14: Water wet system – left, showing a lower contact angle, and oil wet system - right showing a higher contact angle (Crain, 2006)	31
Figure 15: Typical Water/Oil relative permeability curve (Honarpour & Mahmood, 1988).....	34
Figure 16: Asphaltene content measurement setup. The filter paper is placed on top of the conical flask.	41
Figure 17: Bottle tests with heptane and crude mixed in 2:1 and 4:1 ratios to determine the asphaltene precipitation potential.	42
Figure 18: Porosimeter used in the study. The core is placed in the chamber at the top.	44
Figure 19: Schematic of the setup to measure gas permeability of the core samples.	46
Figure 20: Hassler sleeve core holder used for injection tests (for cores up to 3-inches in length).....	50
Figure 21: Vacuum saturation setup. The cores are placed in the conical flask, and the vacuum pump is connected to the flash through a cold trap.	52
Figure 22: Imbibition setup which consists of a Mettler Toledo balance, from which the core sample is suspended in the fluid.	61
Figure 23: Schematic of the brine-heptane relative permeability setup	64
Figure 24: The reservoir top view (left) and side view (right)	65

Figure 25: Permeability and porosity maps of the field grid tops. Higher permeability zones were to the center of the simulated field.	66
Figure 26: Asphaltene precipitation after bottle tests. More precipitation is noted in case of crude mixed with heptane in 1:4 ratio.....	68
Figure 27: Pressure vs. Time for crude injection. The continuous rise in pressure indicates deposition and clogging of the pore spaces.....	69
Figure 28: Cores after crude injection (left) and after heptane flush (right). The darker tones of the cores indicate the presence of crude residue, even after heptane flush.	70
Figure 29: Native permeability's of the core samples ranging from 95-160 md.	72
Figure 30: Permeability of the cores before and after the introduction of asphaltenes. The treated cores showed lower permeability compared to the native state.	75
Figure 31: TOC Measurements of the 3 samples at the inlet, outlet and the center. Vacuum saturation showed a better TOC profile throughout the core.....	77
Figure 32: Comparison of TOC with density values for different cores at the inlet, center and the outlet.....	78
Figure 33: Pressure drops across the cores during brine injection. Higher pressures correspond to a more water wet state.	81
Figure 34: Pressure drop across the cores during heptane injection. Final saturations are also provided to determine the wetting state.	83
Figure 35: Imbibition results with water. The exposed cores showed a lower imbibition rate and imbibition capacity.	86
Figure 36: Imbibition results with heptane. Exposed cores show a more neutral wet state or air-heptane imbibition.	88

Figure 37: Brine-Heptane relative permeability on a clean sample GB-J7-1	91
Figure 38: CMG generated curves for Brine-Heptane relative permeability on a clean sample GB-J7-1	91
Figure 39: Brine-Heptane relative permeability endpoints for core exposed to crude GB-J10-1	92
Figure 40: CMG Generated Curves for Brine-Heptane Relative Permeability on a Core Exposed to Crude GB-J10-1	93
Figure 41: Relative permeability curves for cores GB-J7-1 (clean) and GB-J10-1 (exposed to crude) showing shift in endpoints	94
Figure 42: Cumulative Oil Production, Before and After Relative Permeability Modification	95
Figure 43: Oil Rate, Before and After Relative Permeability Modification	95
Figure 44: Water Rate, Before and After Relative Permeability Modification.....	96
Figure 45: Native case simulation, with no asphaltene precipitation. Shows higher recovery and lower remaining oil saturation	97
Figure 46: Modified case simulation with asphaltene precipitation. Shows lower recovery and higher remaining oil saturation	97

Abstract

Asphaltene precipitation, and the resulting decline in oil production, has for long been identified as a severe problem in oil reservoirs. The deposition of these high molecular weight oil fractions in pore spaces have been known to contribute significantly to permeability impairment and wettability alteration in such reservoirs. Though the phenomenon has been previously studied and documented in several laboratory experiments, many of the results are masked by the limitation of non-uniform asphaltene precipitation throughout the sample, which causes heterogeneities making many of the macroscopic measurements very hard to analyze. As a result, the deposition phenomena in reservoir rock and its impact on rock characteristics and fluid dynamics is still not well-understood and this is the focus of our study.

The development of an experimental workflow to create a uniform deposit of asphaltene inside the core sample is the base line of the initial experiments. This deposit is introduced either through injection of a crude, vacuum saturation or injecting a mixture of heptane and crude. Rock samples from Berea sandstone are prepared and exposed to Texas crude. The deposit uniformity is assured through localized Total Organic Carbon (TOC), permeability and density measurements. The impact of this deposit on the rock wettability is then quantified by measuring the relative permeability endpoints for a brine-oil system in addition to imbibition tests. Wettability alteration is then evaluated, and the results are analyzed in terms of its impact on well operations.

The results show that injecting oil or a heptane-oil mixture results in a non-uniform deposition of asphaltene, which was quantified using the TOC and absolute permeability measurements. Full exposure to crude oil was obtained through vacuum saturation where the asphaltene is deposited uniformly. Deposition of asphaltene molecules, and the subsequent alteration of rock characteristics is evident from the imbibition results where a reduction in both the water imbibition rate and capacity is reported. In addition, the reduction in the absolute permeability could be up to 20% in cores experiencing asphaltene deposition. Core floods results conducted on the exposed rocks indicate a change in the wetting phase properties, with the exposed rocks becoming more mixed/intermediate wet, which is different in the case when the brine saturation is introduced initially to the rock. This in turn impacts the relative permeability of the rocks, and a shift in the end points of the relative permeability curves is noticed. Incorporating this new data in a simulator indicated a disparity in the modeled results before and after accounting for asphaltene deposition.

A workflow was established to achieve uniform deposition of asphaltene in the rock so that enables reliable quantitative measurements of the impact of this deposition on rock characteristics and wettability. Experimental data indicate that there is an alteration in both rock characteristics and relative permeability, and this could be severe and permanent in some cases.

CHAPTER 1: INTRODUCTION

1.1 What are Asphaltenes?

Asphaltene precipitation, and resulting decline in oil production, has for long been identified as a severe problem in oil reservoirs. Asphaltenes can be defined as complex hydrocarbon fractions of crude oil, which are soluble in light aromatics such as toluene, but insoluble in low molecular weight n-alkanes such as heptane and pentane (Mirzayi, Vafaie-Sefti, Mousavi-Dehghani, Fasih, & Mansoori, 2008). These complex organic materials can be further described as polar, poly-aromatic and high molecular weight fractions of crude oil, and are arranged in stacked, multi-ring structures as shown in **Figure 1**. Within the reservoir, they exist either independently as a finely dispersed colloidal suspension in oil stabilized by resins, or are dissolved in the oil (Zhou, 2011). The molar mass of asphaltenes have been reported to range from 1000 g/mol to as high as about 10,000 g/mol (Zanganeh, et al., 2011). At favorable thermodynamic conditions, the asphaltenes are stable and dispersed in the oil, but they can flocculate and precipitate out if thermodynamic instability occurs in the reservoir (Zhou, 2011).

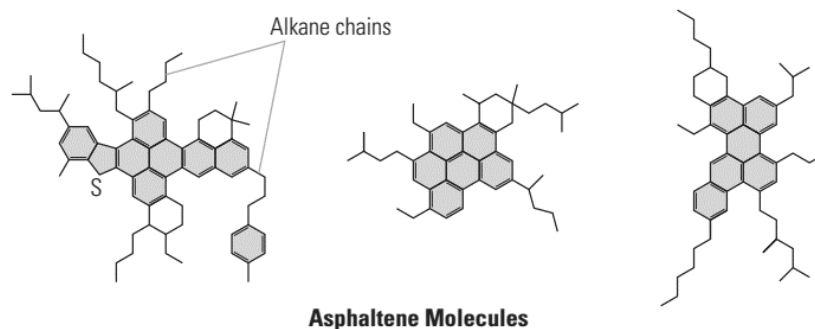


Figure 1: Asphaltene molecules, showing the stacked multi-ring structures (Akbarzadeh, et al., 2007)

The precipitation of these particles has been known to contribute significantly to a variety of problems both in the reservoir and production facilities, including permeability and porosity impairment, altering rock wettability as well as plugging of wellbores, production tubing and equipment (Mirzayi, Vafaie-Sefti, Mousavi-Dehghani, Fasih, & Mansoori, 2008). **Figure 2** shows an example of asphaltene clogging in production pipes, from which it could be seen that deposition could be quite severe. Asphaltene precipitation and deposition during crude oil production is one of the costliest problems facing the industry, and the treatments to remedy this problem increases the operating costs significantly (Zanganeh, et al., 2011).



Figure 2: Asphaltene deposition in pipes (Akbarzadeh, et al., 2007)

1.2 Causes of Asphaltene Precipitation and Factors Affecting the Deposition

Asphaltene precipitation, flocculation and deposition in the reservoir, and production facilities could be triggered by a variety of factors, especially due to any thermodynamic instability induced during the production process. One of the most common reason is the depressurization of the crude oil during the production, resulting

in the flocculation of asphaltenes, and the subsequent deposition. This behavior can be predicted from the phase diagram as shown in **Figure 3**, as per which there is an asphaltene envelope where the chances of these heavier molecular weight components precipitating out is higher. As the pressure declines in the reservoir and as the pressure and temperature falls within this asphaltene envelope, these components precipitate out of the crude oil, leading to flocculation and deposition. Additionally, when external solvents such as Natural Gas Liquids, liquefied petroleum gas, natural gas or other gases like carbon dioxide are used to displace the crude oil during enhanced oil recovery, precipitation of asphaltenes might occur, leading to deposition within the reservoir, and impairment of permeability (Mirzayi, Vafaie-Sefti, Mousavi-Dehghani, Fasih, & Mansoori, 2008).

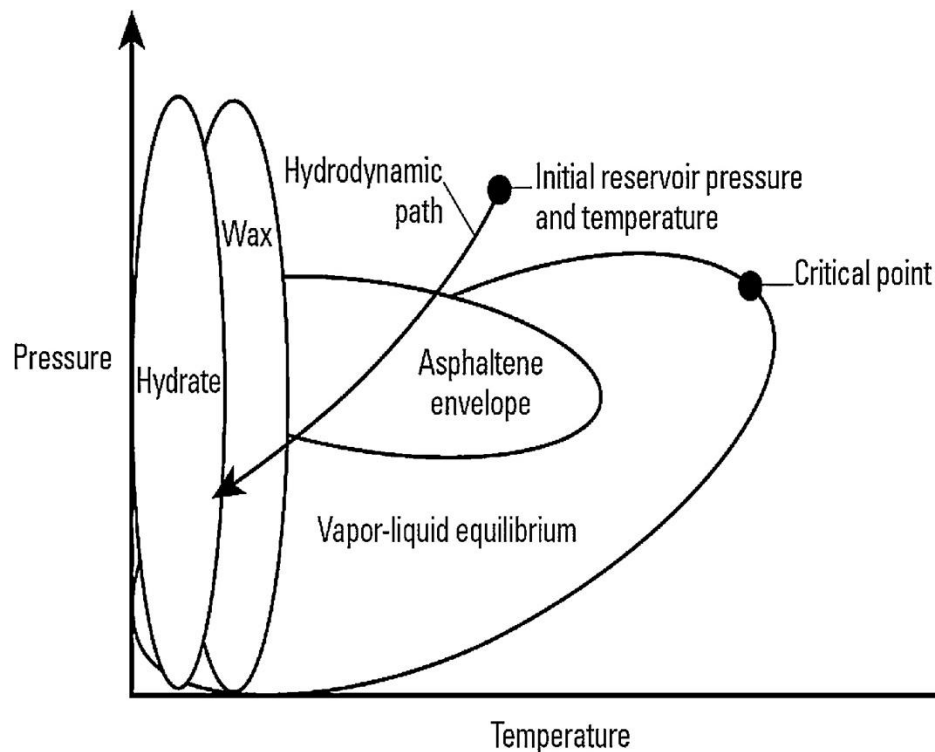


Figure 3: Asphaltene precipitation behavior as shown by a sample phase envelope (Zendeboudi, et al., 2014)

Additionally, certain factors also influence the degree of asphaltene precipitation in porous media and the extent of the problems caused by it. These include the nature, saturation, properties and distribution of the reservoir fluids, as well as the mineralogy and the properties of the reservoir rock. The work done by Mirzayi et. al. (2008) also showed that the amount of precipitation was dependent on the asphaltene content and the presence of resins and waxes in the crude oil. The formation pressure and temperature, as well as the pressure drawdown also impact the extent of asphaltene flocculation (Mirzayi, Vafaie-Sefti, Mousavi-Dehghani, Fasih, & Mansoori, 2008). Zanganeh et. al. (2011) have reported that asphaltene particles tend to flocculate more and create larger particles as temperature increases (Zanganeh, et al., 2011). Additionally, in case of enhanced oil recovery, the nature of the injection fluids, as well as the chemistry of formation brine also impacted the degree of asphaltene precipitation in the reservoir (Mirzayi, Vafaie-Sefti, Mousavi-Dehghani, Fasih, & Mansoori, 2008). Several studies have also focused on the impairment of rock characteristics during miscible or immiscible gas drives, which could potentially lead to asphaltene precipitation and deposition, leading to formation damage (Eskin, Mohammadzadeh, Akbarzadeh, Taylor, & Ratulowski, 2016).

The process of asphaltene deposition, and its impact on reservoir and production performance are relatively well understood. However, the reason why asphaltene precipitation occurs only in some crudes, while others do not produce any precipitation even under similar conditions is still a matter of significant research. Rogel et. al. (2015) observed that it is difficult to link the chemical characteristics of asphaltenes with their solubility and deposition behavior in reservoir rocks. However, they have reported that aromaticity and the hydrogen-carbon molar ratios of the asphaltenes might have a role to

play in dictating which crudes might encounter asphaltene precipitation (Rogel, Miao, Vien, & Roe, 2015). Eskin et. al. (2016) in their paper also mentioned that asphaltene precipitation can be seen in both heavy and light crudes, and that both field and experimental data showed that the solubility of asphaltenes is generally lower in lighter crudes. Hence, they concluded that asphaltenes have a higher tendency to precipitate due to depressurization or gas injection in lighter oils compared to heavier crudes. They also pointed out the example of the Venezuelan Boscan Crude, which has 0.172 g/g of asphaltenes, and was produced by pressure depletion without experiencing any asphaltene precipitation issues, while the crude from Hassi-Messaoud field in Algeria, which has only 0.0015g/g of asphaltene has experienced severe production problems due to asphaltene precipitation on pressure depletion (Eskin, Mohammadzadeh, Akbarzadeh, Taylor, & Ratulowski, 2016).

1.3 Deposition Mechanism

Reservoirs with even minute content of asphaltene are susceptible to asphaltene precipitation not only through pressure depletion during primary recovery, but also through compositional change of the reservoir fluid. Experimental results have shown that the region of asphaltene instability would be located between the AOP and just above the bubble point pressure, and that denser asphaltenes have a higher tendency to precipitate compared to lighter asphaltenes (Eskin, Mohammadzadeh, Akbarzadeh, Taylor, & Ratulowski, 2016). Asphaltene deposition follows two mechanisms – aggregation of asphaltenes, followed by the deposition and plugging of asphaltenes. This can be seen in **Figure 4** and **Figure 5**. The first mechanism is the aggregation of the

asphaltene molecules, during which the dissolved asphaltene nano-aggregate particles start to clump together, resulting in their size to increase from less than 3 microns to more than 1 micron. As the clumps grow larger, they become more solid like with aging, resulting in the molecules precipitation out of the crude solution. Following this, as shown in **Figure 5**, is the deposition and plugging mechanism. Precipitated asphaltenes may continue to flow as suspended particles, or may flocculate further and deposit on the reservoir rock, leading to permeability impairment and wettability alteration. This begins with the adsorption of flocculated asphaltene particles onto active sites on the rock surface, particularly in areas of high clayey minerals such as kaolinite (Dahaghi, Gholami, Moghadasi, & Abdi, 2008). This behavior can be attributed to the polarity of the asphaltene molecule, and because of its stacked and multi-ring structures due to which, the polar ends interact with the clay molecules (Ju, Qiu, Qin, Chen, & Fan, 2010).

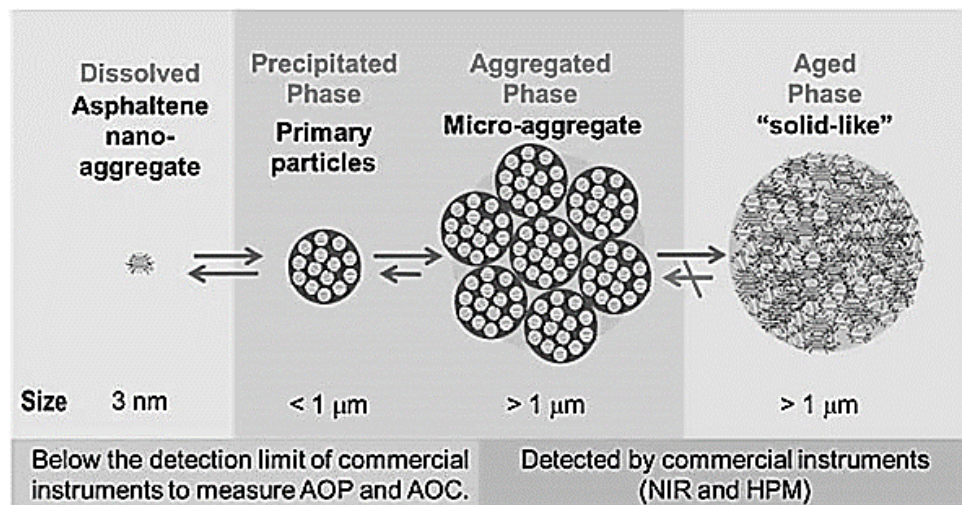


Figure 4: Asphaltene aggregation mechanism based on the Yen-Mullins model showing the clumping of asphaltene molecules (Vargas, et al., 2014)

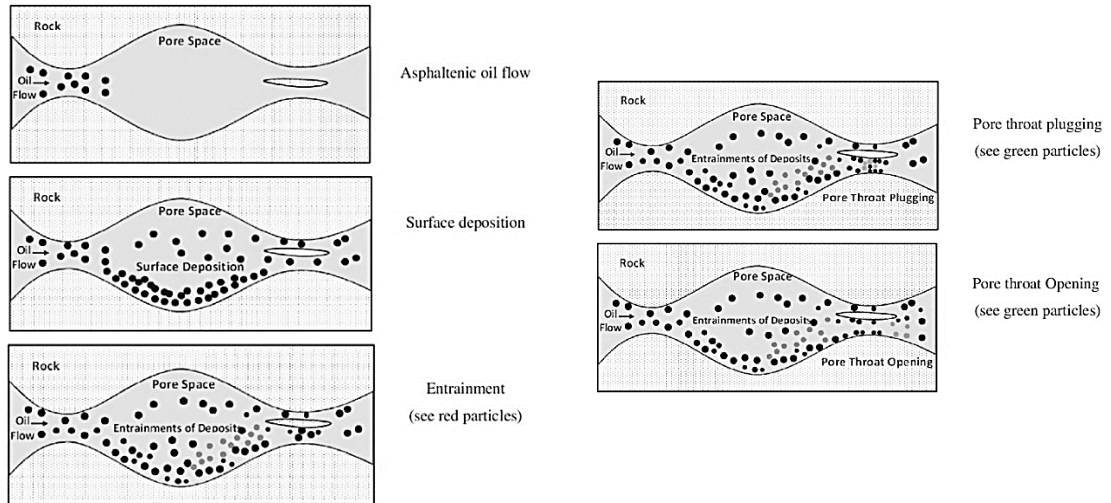


Figure 5: Asphaltene deposition and plugging mechanism (Kord, Mohammadzadeh, Miri, & Soulgani, 2013)

The larger and high molecular weight asphaltene particles are then retained hydrodynamically, or trapped in the pore throats, thereby restricting flow and leading to a reduction in the pore spaces available for the reservoir fluids. Other problems that could arise from this include formation damage due to permeability impairment, and due to the alteration of the rock wettability from water-wet to oil/mixed-wet. Dahaghi et. al. (2008) has also mentioned that this mechanical entrapment can cause up to 70% permeability reduction in the reservoir (Dahaghi, Gholami, Moghadasi, & Abdi, 2008).

1.4 Problems Caused by Asphaltenes

While the precipitation of asphaltenes in-situ in the reservoir could have some advantages such as an increased production share of lighter and less viscous crude, reduced asphaltene precipitation in production lines, and the need for increased crude oil processing; it is generally considered as a significant and persistent problem, which damages the reservoir and impairs production in the long term (Mukhametshina, Kar, & Hascakir, 2015).

Among the most significant of issues due to asphaltene precipitation and deposition in-situ in the reservoir is the reduction of the porosity and permeability. Asphaltene molecules tend to aggregate, precipitate and deposit onto surfaces, and given their large sizes, can clog pore spaces and act as a significant impediment to flow. Additionally, the deposition of asphaltenes to the rock surface can alter the wettability of the rock and thereby change the relative permeability from water-wet to an oil-wet or a mixed-wet system (Khanifar, Onur, & Darman, 2014). This can reduce the oil recovery efficiency severely, and cause formation damage. Wettability changes can also give rise to other problems such as poorer performance when improved oil recovery techniques such as water flooding is implemented (Dahaghi, Gholami, Moghadasi, & Abdi, 2008). Blunt et. al. (2012) in their paper, noted that field trials on asphaltene precipitation highlighted a significant decrease in well productivity of about 10%, and the near wellbore skin increased from 0 during a low production test to about 0.6 in a high production test. Asphaltene interactions with formation brine could also raise additional problems from the formation of oil-water emulsions leading to wellbore clogging (Blunt, et al., 2012).

Additional problems due to asphaltene precipitation include clogging of the subsurface equipment, as well as the production and transmission lines, especially during the transportation of crude, and during processing in the refinery (Mukhametshina, Kar, & Hascakir, 2015). Signs of asphaltene deposition outside the reservoir first appear in surface facilities such as the separators and tanks, and this can cause considerable damage to such equipment. Asphaltene precipitation can also occur within the production tubing at depths corresponding to the Asphaltene Onset Pressure (AOP) of the reservoir, causing electrical submersible pump failures, block sand screens, tubing plugging, wellhead freezing and in cases of severe deposition, a significant reduction of well productivity and injectivity. Zekri et. al. (2009) also observed that crudes with high sulfur content showed larger sulfur precipitation on the onset of asphaltene deposition, leading to more noticeable plugging and reduced productivity (Zekri, Shedid, & Almehaieb, 2009).

Since asphaltene precipitation impacts all parts of an oil field operation from well tubing to the flow lines, the production separator, and other downstream equipment, the problems associated with it are also expensive to remediate (Leontaritis & Mansoori, 1988). This increases the operating costs due to the need for cleanup treatments, as well as due to the loss of production because of having to shut in the well to mitigate these issues (Rogel, Miao, Vien, & Roe, 2015). Zhou (2011), in his thesis, estimated the cost for asphaltene cleaning workover could be as high a \$500,000 for an onshore well and \$3 million for an offshore well (Zhou, 2011). Hence, the downtime, cleaning, and maintenance costs are a sizable factor in determining the economics of producing from a field prone to asphaltene deposition (Leontaritis & Mansoori, 1988).

1.5 Field Examples

Asphaltene deposition, and the problems associated with it are experienced in reservoirs around the world, as per Stankiewicz (2011) and as shown in **Figure 6**Figure 6: Asphaltene content of some crudes from around the world . However, only some countries have serious challenges with asphaltenes such as Venezuela and Kuwait (Stankiewicz, 2009).

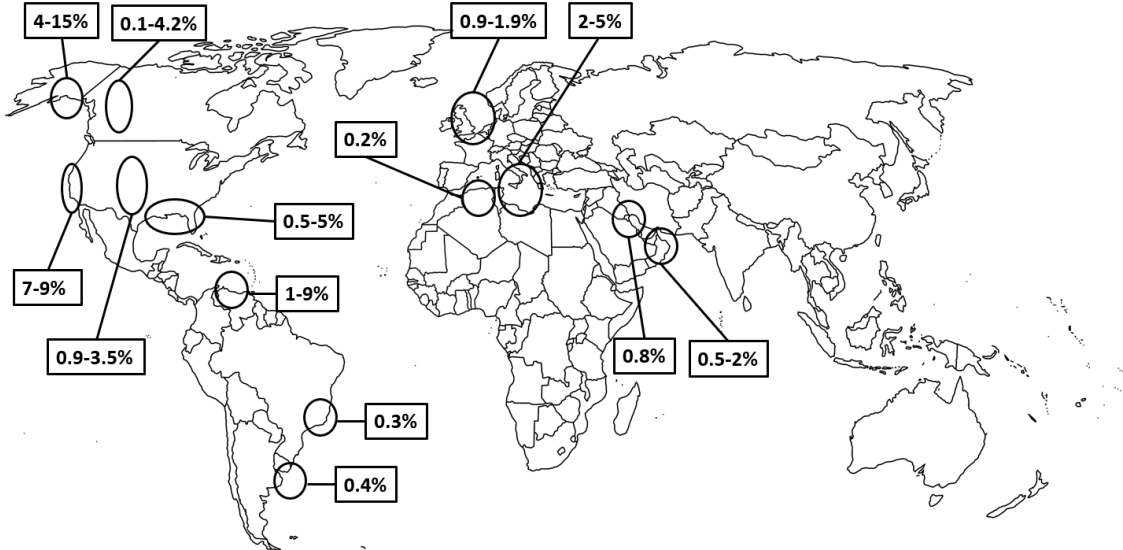


Figure 6: Asphaltene content of some crudes from around the world (Stankiewicz, 2009)

1.5.1 Abu Dhabi

Zhou (2011), in his thesis research, studied a test field in Abu Dhabi which was experiencing problems with asphaltene precipitation. The field had a tar mat which covered about one third of the field, and it was also noticed that the asphaltene concentration in the oil increased with depth. Because of the presence of the tar mat, and the high asphaltene content in the crude, the operating expenditure (OPEX) of the field

was significantly higher. The field could also not be subjected to gas injection to offset production decline, as there was the possibility of an increase in the asphaltene precipitation. The field and the production facilities also experienced flow assurance issues, especially in the field flow lines (Zhou, 2011).

1.5.2 Rhourd-Nouss Sud Est Field, Algeria

Experimental study conducted by Amroun & Tiab (2001) on the Rhourd-Nouss Sud Est Field in Algeria showed that asphaltenes precipitated out of the crude and played a significant role in altering the wettability of the reservoir rock. They claimed that the higher concentrations of asphaltenes shift the rock towards more intermediate and neutral wetting state, compared to the earlier state. They also suggested that the extent of wettability alteration depends on the concentrations of asphaltenes in the crude oil, and that alteration of wettability in the field due to this precipitation and deposition is irreversible (Amroun & Tiab, 2001).

1.5.3 Prinos Field

In the Prinos Field in the north Aegean Sea, severe asphaltene deposition led to wells completely ceasing to flow in few days, after having initial production rate of up to 3000 barrels per day. The problem of asphaltenes precipitating out in Prinos field was so severe that it was considered that the project might not be economically viable. Precipitated asphaltenes, in many instances carried from the well tubing to the flow lines, the production separator and other downstream equipment, and thereby damaging these equipment. This leads to severe economic implications, especially considering that the cleanup and workover costs for these wells could go up to \$250,000. Several mediation

efforts were conducted including injecting solvents such as xylene to prevent and remedy the deposition problem (Leontaritis & Mansoori, 1988).

1.5.4 Hassi Massaoud Field, Algeria

Asphaltene deposition in the wells and tubing was a serious production problem in Hassi Massaoud, and several intervention methods were needed to continue maintaining production from the field. The wells in Hassi Massaoud field in Algeria experienced a significant loss in well head pressure (about 20-25%) within 15-20 days after the onset of asphaltene precipitation, which led to a loss in production (Leontaritis & Mansoori, 1988). Additionally, the deposits of asphaltenes on the tubing's were so severe that the tubulars had to be frequently washed or scraped to remove these deposits. Most of the deposition in the tubing's were noticed in the pressure region just below the bubble point pressure. A significant program to monitor the pressure of the well, along with frequent washing of the tubulars was employed to counter the problem of asphaltene deposition (Haskett, Tartera, & Polumbus, 1984)

1.5.5 Magwa Marrat Reservoir, Kuwait

Blunt et. al. (2012) studied the effects of asphaltene deposition in the Magwa Marrat reservoir in Kuwait. Due to severe asphaltene precipitation issues, the wells in the field had to undergo periodic cleaning and solvent jobs with toluene and diesel to remove the deposited asphaltenes. The asphaltene deposition in the reservoir also led to a direct loss in oil recovery, but noted that the loss was minor since the asphaltene constituted only 0.2% by weight of the reservoir oil. Field trials also showed a significant decrease in well productivity of about 10%, and an increase in the near wellbore skin. The reservoir

also showed signs of permeability damage and wettability changes, as well as problems with oil-water emulsions clogging the production facilities (Blunt, et al., 2012).

1.6 Industry Methods to Mitigate Asphaltene Problems

A variety of techniques have been employed or developed by the industry to address the problem of asphaltene precipitation and deposition, depending on the location and the severity of the deposition. Asphaltene precipitation is broadly tackled in two ways: by inhibiting the precipitation, or by employing removing methods. Adjusting the production processes during well design stage to avoid asphaltene dropout has been considered as the best solution considering the economical, technical and environmental criteria. This includes adjusting the wellhead pressures to keep it above the Asphaltene Onset Pressure (AOP), shear reduction, removing incompatible materials from mixing with the crude, ensuring pressure maintenance in the production facilities as well as neutralizing the electro static forces in the pipes. All these are aimed at preventing the produced crude from entering the thermodynamic instability zone of asphaltene precipitation (Hasanvand, Ahmadi, & Behbahani, 2015).

Typical solutions for removing methods include the use of solvents, chemical inhibitors and pyrogenics, as well as ultrasound methods (Kazemzadeh, Malayeri, Riazi, & Parsaei, 2014). The use of aromatic solvents such as xylene and toluene are most common, since the asphaltenes are soluble in these and can avoid or delay the in situ Asphaltene precipitation (Mukhametshina, Kar, & Hascakir, 2015). However, these techniques cannot be generalized for every well and reservoir, and the high price tag,

damaging environmental impacts and poor efficiency are among the reasons that prevent their widespread utilization (Kazemzadeh, Malayeri, Riazi, & Parsaei, 2014).

Advances in nanotechnology can also provide some opportunities to tackle the challenges caused by asphaltene deposition, and work done in several studies have shown that the injection of nanoparticles can improve operational performance through wettability alterations, reducing interfacial tension and reducing oil viscosity and improving mobility. Kazemzadeh et. al. (2014) used Fe_3O_4 nanoparticles to reduce the intensity of the asphaltene precipitation by altering the interfacial tension. However, even though it has been shown to work in the lab, research has not been done on its implementation on a field scale, and how the results would vary (Kazemzadeh, Malayeri, Riazi, & Parsaei, 2014).

CHAPTER 2: LITERATURE REVIEW

Asphaltene precipitation, and the resulting formation damage to the reservoir has been a topic that has constantly been studied actively in the laboratory. The results from these studies are either based from experiments using real cores, porous media or other models using tubes or well characterized particles, as well as modeling studies. Studies have generally focused on the permeability impairment due to asphaltene deposition because of pressure depletion below the Asphaltene Onset Pressure (AOP) or because of compositional changes in the reservoir fluid due to IOR or EOR processes (Eskin, Mohammadzadeh, Akbarzadeh, Taylor, & Ratulowski, 2016).

To determine the formation damage that occurs naturally because of pressure depletion, Minssieux (1997) conducted core flood experiments on sandstone samples with different crude oils, and the formation damage caused by asphaltenes was evaluated by permeability measurements using cyclohexane. The results indicated that there was 20-90% drop in the permeability compared to the initial values, but this depended on the rock mineralogy and asphaltene content (Minssieux, 1997). Results of permeability reduction from another paper by Minssieux et. al. (1998) is shown in **Figure 7**. However, the author did not consider the impairment mechanism involved during the study, and the test conditions were limited to the ambient conditions (Minssieux, Nabzar, Chauveteau, Longeron, & Bensalem, 1998). Similar experiments were also conducted by Eskin et. al. (2016) on carbonate rocks to determine how asphaltene deposition affected the carbonate rock permeability. The tests were run until the pressure drop across the core stabilized, or if the injection pressure became too high. The authors also noted that permeability impairment was indeed due to asphaltene deposition by analyzing the asphaltene content

of oil at both the inlet and effluent streams of crude (Eskin, Mohammadzadeh, Akbarzadeh, Taylor, & Ratulowski, 2016).

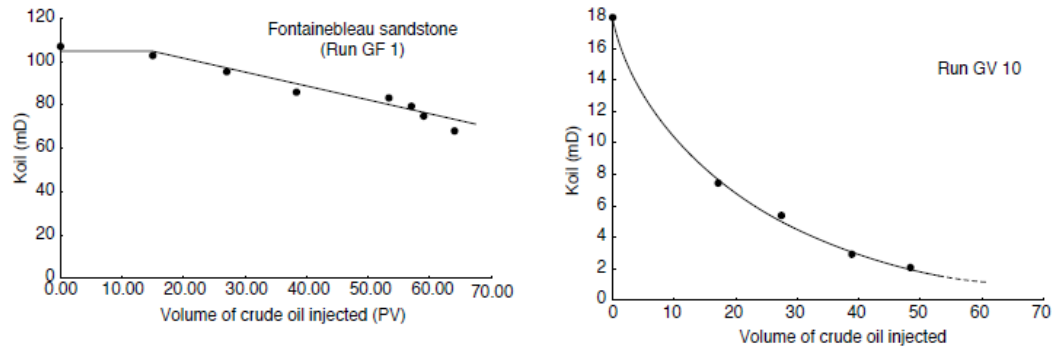


Figure 7: Oil permeability reduction in Fontainebleau and Vosges sandstones following injection with crude (Minssieux, Nabzar, Chauveteau, Longeron, & Bensalem, 1998)

Kocabas (2003) conducted similar experiments by using a crude sample from the UAE and asphaltene deposition was studied in carbonate rocks using Scanning Electron Microscopy measurements. Based on these, the author noted that approximately 80% of the deposition occurred in the first 1/3rd of the core length, indicating that the deposition of asphaltenes in the core by injection is not uniform. It was also noted that 60-80% of the permeability reduction could be reversed by changing the flow direction, indicating that damage was mainly due to pore throat blocking, rather than mainly by deposition and adsorption of asphaltene particles on the rock surface (Kocabas, 2003). Shedid and Abbas (2005) also performed experiments to quantify the adsorption of asphaltenes on rock surfaces during primary production. They determined that static adsorption on rock surfaces consumed about 40% of the initial asphaltene content of the crude, while dynamic adsorption in the porous medium reduced the asphaltene content in the crude by about 80%. In addition, they also reported that asphaltene deposition caused a more

severe formation damage in low permeability rocks, compared to higher permeability one (Shedid & Abbas, 2005).

Core flood tests were also conducted by Del la Cruz et. al. (2009) to investigate the effects of pressure drop, flow rate, effective porosity and initial absolute permeability on altering the rock characteristics of a limestone sample, with a crude collected from Mexico. The tests were conducted at reservoir temperature indicating that permeability reduced by about 24% after injecting 34 pore volumes of crude at below the Asphaltene Onset Pressure (AOP). However, the tests conducted through crude injection tended to have higher concentration of the deposited asphaltenes at the face exposed to flow initially (De La Cruz, Argüelles-Vivas, Matías-Pérez, Durán-Valencia, & López-Ramírez, 2009). Rezaian et. al. (2010) also performed asphaltene impairment studies on sandstone samples through core flood tests at different injection flowrates and asphaltene concentrations where permeability impairment was studied as a function of the differential pressure across the core sample. Though the results showed a significant impairment in permeability, the authors observed that most of the deposition was on the injection face, and did not report on how significant the asphaltene deposition inside the core matrix impaired the permeability (Rezaian, et al., 2010).

Mirzayi et. al. (2008) also studied the effects of asphaltene deposition on unconsolidated porous media using an Iranian crude oil sample, which had about 6.56% asphaltene by weight. Porosity and permeability reduction was measured to determine the impact of asphaltene deposition, and wettability alteration was measured by the changes in the volumes of the irreducible water, and the cumulative water produced. The study showed that there was porosity and permeability reduction, and the volume of

irreducible water decreased from 26.5% to 10.7% after injection, indicating a change in wettability from an initial water wet. However, it has been shown that using irreducible volume as a method to establish wettability change can be highly inaccurate and cannot be used to determine localized alterations (Mirzayi, Vafaie-Sefti, Mousavi-Dehghani, Fasih, & Mansoori, 2008).

Injecting gases into oil reservoirs to enhance reservoir productivity can also cause asphaltene impairment issues due to compositional changes in the reservoir fluids. CO₂ injection is one of the main processes that induces asphaltene precipitation, especially when its concentration exceeds the critical value determined by fluid composition, temperature and pressure. CO₂ injection core flood experiments done by Sims et. al. (2005) showed that there was significant blocking at the injection faces of carbonate cores at a higher concentration of CO₂ injection, with permeability reduction in the range of 32-50% when injected with oil containing 0.6 mol/mol of CO₂ (Sim, Okatsu, Takabayashi, & Fisher, 2005). However, the results were inconclusive when other gases like natural gas are used for injection. Hayashi and Okabe (2010) showed that while asphaltenes were selectively deposited near the inlet of the core for CO₂ injection, the deposited particles were more uniformly distributed for hydrocarbon gas injection, and that while CO₂ injection caused a 20% permeability reduction, the permeability reduction by hydrocarbon gases was negligible (Hayashi & Okabe, 2010). Dehgani et. al. (2007) also conducted asphaltene impairment studies on packed cores during natural gas injection by measuring the asphaltene content of the produced oil, and noted that it decreased suddenly upon starting the injection, and then increased gradually to reach the level of the injection oil, indicating that adsorption onto the rock surface was finished.

After measuring permeability, porosity and ageing, it was determined that there was an increase in asphaltene deposition leading to pore plugging, porosity reduction and absolute permeability damage. It was also argued that the cores changed wettability to oil wet due to natural gas induced asphaltene precipitation and deposition. However, no independent attempt was made to verify this, and there was no evidence presented on the initial wettability state of the packing materials used in the core (Dehgani, Ali, Vafaie-Sefti, Mirzayi, & Fasih, 2007).

Consistent results were obtained when Hopkins et. al. (2016) in their research, considered the adsorption of acidic crude oil components on limestone samples at different wetting conditions. The crude which they used was diluted with heptane in a 60:40 ratio, and no asphaltene precipitation was observed. However, flooding with crude reduced the water wet surface of the limestone sample, and the water-wet surface area further reduced when the core was aged for two weeks. These results were confirmed using spontaneous imbibition tests and this was attributed to the adsorption of acidic polar components of crude oil on the rock surface. Since Hopkins et. al. (2016) did not measure the initial asphaltene content of the crude, and since they relied only on observing if there was precipitation of asphaltene, results of this study are questionable as this wettability modification could also be due to asphaltenes, which are acidic and polar in nature (Hopkins, et al., 2016). Shabib-Asl et. al. (2015) also focused on similar areas where they quantified wettability alteration of Berea sandstone using crude having different acid and base numbers. Their study determined that the magnitude of change of wettability is dependent on the concentration of polar components in the crude, and crude having a

higher Total Base Number (TBN) showed a higher change in wettability from oil to water wet, and vice versa (Shabib-Asl, Ayoub, Saaid, & Valentim, 2015).

Wolcott et. al. (1996) in their research also considered the relation between wettability alteration and the oil asphaltene and resin content. Experiments were conducted on Berea sandstone cores, with six different crude oils. The cores were initially saturated with brine (5% NaCl) before being flooded with oil, and then aged for a week, followed by a flush with hexadecane before measuring wettability's using the Amott method. The results from their works showed a positive relation between wettability alteration and the asphaltene and resin content, as well as with the extent of adsorption. They also suggested that the presence of brine inhibited organic deposition and limited wettability alteration from water wet to oil wet (Wolcott, Groves, & Lee, 1996). Jia, Buckley and Morrow (1991) also did similar studies using Berea cores which were saturated with brine, flushed with crude oil, and then aged at different temperatures, before the wettability alteration was assessed by the Amott method. Two crude samples were used, Moutray crude, and North Sea crude, and the cores were aged for 1-20 days at temperatures ranging from 22-80 degrees Celsius. Wettability change was noticed in the cores, and the degree of change to neutral or oil wet increased as the flushing volume of crude and the aging time increased, while it decreased as the temperature increased. The study also reported that the wetting alterations persisted over a storage period of 2 to 6 months (Jia, Buckley, & Morrow, 1991).

Hematfar et. al. (2013) investigated the change in two-phase flow behavior, displacement performance, relative permeability and recovery due to asphaltene precipitation and deposition. Their experiments were done on sand packs, and asphaltene

from Canada mixed with toluene was used instead of a crude sample, along with brine as the second phase. Tests were done to determine the effect of salinity, and asphaltene concentration on relative permeability and recovery, as shown in **Figure 8**. A shift in the end points was observed when the cores were saturated with crude, and there was adsorption of asphaltenes onto the surface (Hematfar, Maini, & Chen, 2013).

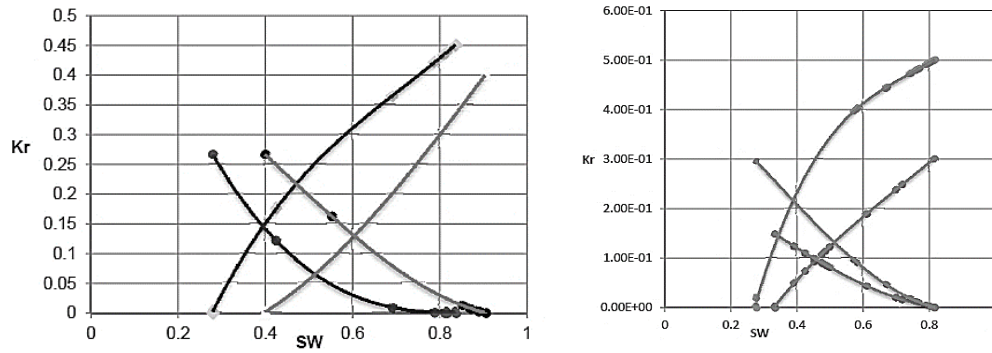


Figure 8: Relative permeability curves pre- and post-adsorption stages showing a shift in the endpoints (Hematfar, Maini, & Chen, 2013)

Comparable results were obtained by Shedid (2001) in his research, which was done with carbonate rocks and three different crudes with different asphaltene contents (0.06-1.5%). The cores were flooded with crude, and then flushed with cyclohexane to determine permeability reduction. Relative permeability is calculated after the core is completely saturated again with crude, and water is injected until no more oil is produced. Based on the results as shown in **Figure 9** and **Figure 10**, Shedid concluded that the permeability drop is higher in case of crude with higher asphaltene content. The relative permeability endpoints are also shifted further depending on the asphaltene content, with the crude having a higher asphaltene content showing a lower irreducible water saturation. Asphaltene precipitation also improves water relative permeability, and

therefore accelerates the water breakthrough during waterflooding of reservoirs with higher asphaltene content (Shedid, 2001).

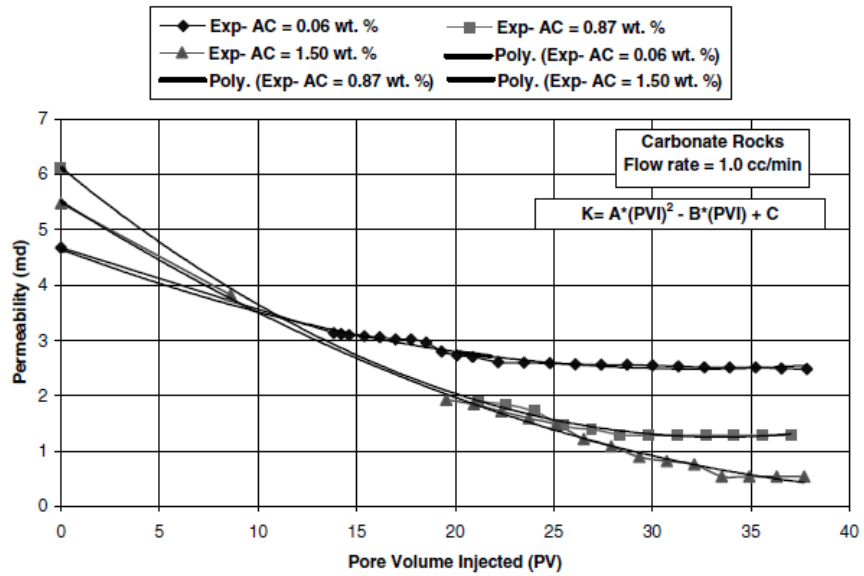


Figure 9: Influence of asphaltene deposition on permeability of core samples for oils with different asphaltene contents (Shedid, 2001)

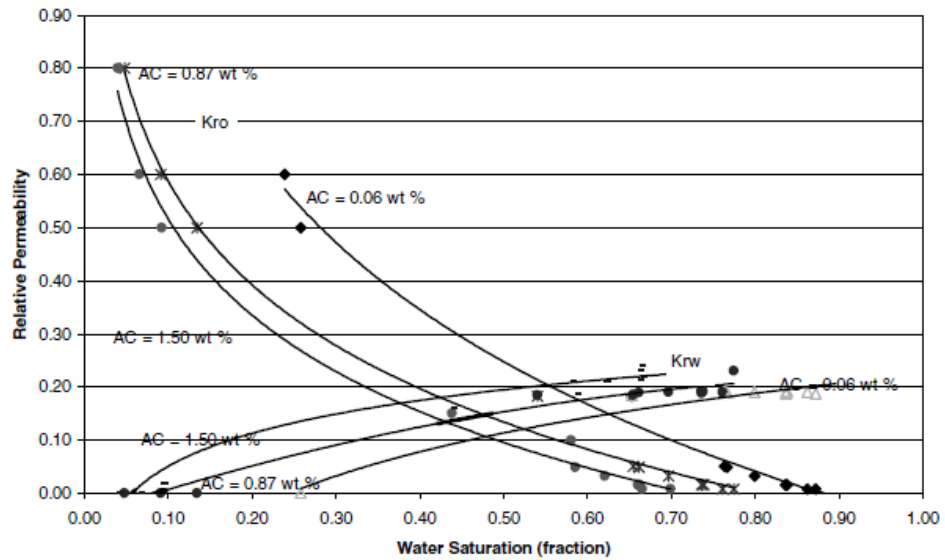


Figure 10: Influence of asphaltene deposition on relative permeability curves for cores created with different crudes (Shedid, 2001)

Nasri and Dabir (2009) further investigated the effects of asphaltene deposition on average reservoir pressure, bottom hole pressure and the water breakthrough using a simulator. This was done based on experimental data including oil and water relative permeability modifications due to asphaltene precipitation. Carbonate cores were used for the experiments, and the relative permeability modifications were evaluated during imbibition and drainage processes. Based on the results obtained during their study, asphaltene deposition leads to higher capillary pressure during drainage, because of which the water relative permeability would be high indicating the rocks are intermediate oil wet with higher amounts of residual oil. When simulated, the results indicated that the cumulative production and the bottom-hole pressure dropped as the asphaltene content increased, as shown in **Figure 11** (Nasri & Dabir, 2009).

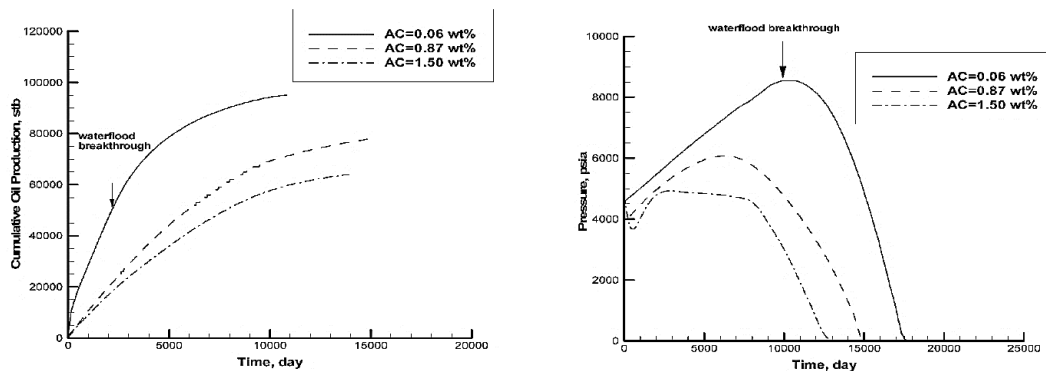


Figure 11: Influence of crudes with different asphaltene content on cumulative oil production and bottom-hole pressure of a reservoir (Nasri & Dabir, 2009)

In summary, even though there is a lot of research being done on this subject, there are issues associated with a lot of the literature which makes some of the conclusions questionable, as well as a lot of dimensions to the problem that are unexplored. A lot of studies did not account for proper ageing of the porous media with the crude, or use a proper chemical agent to flush out the excess crude from the rock without causing further

destabilization, or removing the asphaltenes already clogging the pores. Also, the effects of localized deposition on the core faces was also not accounted for, which can lead to inaccurate results. Asphaltene deposition at the inlet of the porous medium can form a filter which can lead to a plugging of the inlet flow path, which is not asphaltene impairment, but a filtration problem (Eskin, Mohammadzadeh, Akbarzadeh, Taylor, & Ratulowski, 2016)

CHAPTER 3: CONCEPTS AND THEORETICAL BACKGROUND

The experiments done during this study made use of several concepts to evaluate the results, from measuring the asphaltene content to evaluating the relative permeability and recovery factor.

3.1 Asphaltene Content Measurements

Since asphaltenes are the oil fractions that are soluble in aromatic solvents such as toluene, and insoluble in paraffinic solvents such as heptane, this definition is used to separate out the asphaltenes in a crude sample, and determine the asphaltene content of the crude. Crude sample is mixed with heptane, and asphaltenes are separated on a filter paper. Based on the ASTM IP143 standard, the asphaltene content, A, in percentage weight is calculated by the following (ASTM International, 2005):

$$A = \frac{M}{G} * 100 \quad (1)$$

Where,

M = Mass of asphaltenes, in grams

G = Mass of the crude used, in grams

The mass of asphaltenes, M, is obtained by measuring the weight of the filter paper, before and after the test, once it is dry.

$$M = Wt. Filter\ paper_{after} - Wt. Filter\ paper_{before} \quad (2)$$

The asphaltene content measured is reported as wt.%, as gram/gram or milligram/gram, and is rounded to the nearest 0.05% (ASTM International, 2005).

3.2 Porosity

Porosity of a core is a measure of the pore volume of the core sample, which could be empty, or filled with a fluid. There are two measures of porosity – absolute and effective. Absolute porosity refers to the total pore volume of a rock, whereas only the interconnected pore volume is considered when measuring effective porosity. Porosity measurements were done in lab, using a setup which works based on Boyle’s law. The law states that the absolute pressure exerted by a given mass of ideal gas in a closed system is inversely proportional to the volume occupied by the same gas at isothermal conditions. This can be represented as:

$$P \propto \frac{1}{V} \quad (3)$$

This can also be written in a different form for a closed system.

$$P_1V_1 = P_2V_2 \quad (4)$$

Where,

P_1, P_2 : Pressure exerted by the gas at various stages

V_1, V_2 : Volume of the gas at various stages

This principle is used to measure the pore volume of the core sample in the lab. The porosimeter has a known volume, and the pressures are noted before and after the core is loaded. The difference in volume is used to calculate the pore volume (V_p) of the core samples. Porosity is then calculated by:

$$\phi = \frac{V_p}{V_B} \quad (5)$$

$$V_B = \frac{\pi D^2 h}{4} \quad (6)$$

Where,

ϕ : Porosity, expressed as a fraction or percentage

V_p : Pore volume, in cm^3

V_B : Bulk volume, in cm^3

D: Diameter of core sample, in cm

h: Length of core sample, in cm

3.3 Permeability

Permeability, as defined by Darcy's law, is a measure of the capacity of a porous medium to transmit fluids through it. It is a complex property that is dependent on many rock properties such as the porosity, grain size, grain sorting, and the size and number of connected pores which are open to flow. Calculating permeability involves the use of Darcy's law, which incorporates the fluid flow rate, viscosity, the length of the porous media and the pressure gradient applied.

$$k = -\frac{q \mu dL}{A dP} \quad (7)$$

Where,

k : Permeability of the porous media, in Darcy (D)

q : Flow rate, in cm^3/s

A: Area, in cm^2

μ : Viscosity, in centipoise (cp.)

dL: Length of the porous media, in cm

dP: Pressure drop across the porous media, in atm.

For the measurement of permeability, nitrogen and helium was used in the lab. However, it is much more difficult to determine gas permeability than liquid permeability using Darcy's law since gases behave differently at pore scale, and so it requires the modification of the general Darcy equation. This equation is represented by:

$$q = A \frac{k}{2\mu P_0} \frac{P_1^2 - P_2^2}{dl} \quad (8)$$

Where,

q : Gas flow rate, in cm^3/sec

A : Area of the porous surface, in cm^2

k : Permeability of the porous media, in Darcy (D)

μ : Viscosity, in centipoise (cp.)

P_0 : Reference pressure, in atm.

dL : Length of the porous media, in cm.

P_1 : Inlet pressure, in atm.

P_2 : Outlet pressure, in atm.

To determine the permeability, it is better to utilize a range of flow rates, and making a plot of $\frac{q}{A}$ versus $\frac{P_1^2 - P_2^2}{2dl}$. Permeability can easily be calculated from the slope of the resulting plot. However, it should be noted that Darcy's law is only applicable when the flow through the material is laminar. At higher flow rates, due to energy losses associated with turbulent flow, a deviation in the slope is noted, and it will no longer be a straight line, as shown in **Figure 12**. Darcy law is not designed to work at these higher

flow rates, and in regions of non-Darcy flow, a different model is required to reliably measure permeability.

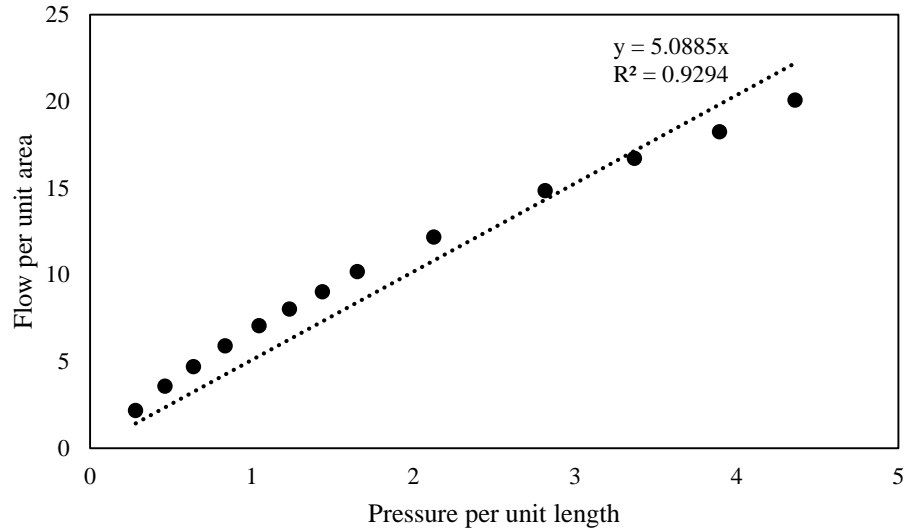


Figure 12: An example calculation of permeability using Darcy equation shows deviation from linear trend in lab experiments. Higher flow region at the top right.

For this purpose, the Forchheimer equation for non-Darcy flow in porous media was used. Forchheimer proposed an equation which can describe the fluid flow at higher velocities, at regions where the Darcy equation fails. For a homogenous, steady flow of an incompressible fluid through a porous media, Forchheimer equation can be noted as:

$$\frac{P_1 - P_2}{\mu L v} = \frac{\beta \rho v}{\mu} + \frac{1}{k} \quad (9)$$

Where,

β : Forchheimer coefficient

P_1 : Inlet pressure, in atm.

P_2 : Outlet pressure, in atm.

μ : Viscosity, in centipoise (cp.)

L: Length of the porous media, in cm.

v : fluid flow velocity, in cm/s

ρ : Density of the fluid, in gm/cm³

k: Permeability, in D

At higher flow rates, a plot of $\frac{P_1 - P_2}{\mu L v}$ versus $\frac{\rho v}{\mu}$ will be linear, and the slope will give the value of β , while the intercept will give $\frac{1}{k}$, from which the permeability could be calculated (Huang & Ayoub, 2008). An example of this is shown in **Figure 13**. In our study, the values of permeability calculated at low flow rates using Darcy's equation mostly agreed with the permeability calculated at higher flow rates using Forchheimer equation, and this was used to evaluate the reliability of the permeability data.

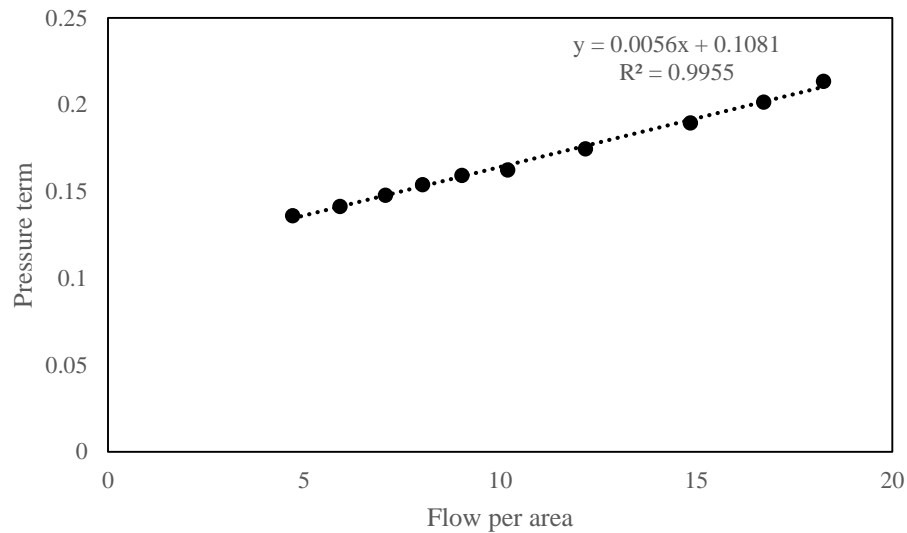


Figure 13: Calculation of permeability of our samples using Forchheimer equation for the non-Darcy region

3.4 Wettability and Spontaneous Imbibition

Wettability is defined as the tendency of one fluid to spread on or adhere to the surface of a solid in the presence of another immiscible fluid. It is due to the interaction between the solid and fluid phases, and depends on the rock surface, as well as the chemical composition of the fluids (Crain, 2006). Measurement of wettability requires micro-scale laboratory investigation, and it can be influenced by the asphaltene content of the oil, salinity of the water, surface roughness and surface free energy. The reservoir rock can be oil wet, water wet, neutral wet or mixed wet depending on these interactions, and can generally be classified by the contact angle of the fluid with the solid phase as shown in **Figure 14**, or through measurements of interfacial tension. During the experiments conducted as part of this study, a change in wettability from water wet to mixed wet, or from oil wet to mixed wet was observed, and this was quantified by the imbibition and relative permeability measurements.

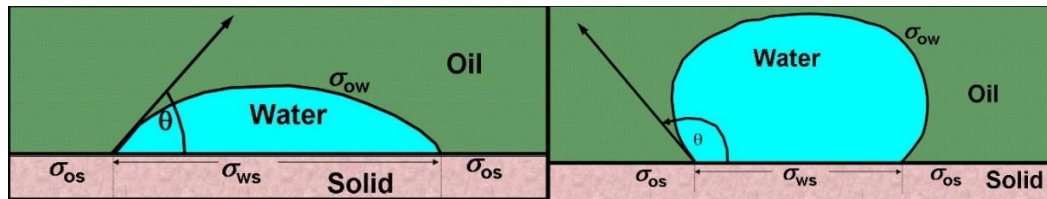


Figure 14: Water wet system – left, showing a lower contact angle, and oil wet system - right showing a higher contact angle (Crain, 2006)

Imbibition is a fluid flow process during which the saturation of the wetting phase increased, and the saturation of the non-wetting phase decreases. During imbibition, a water-wet rock which is saturated with oil will imbibe water into its pores when placed in a bowl of water, and an oil wet rock, which is saturated with water will imbibe oil to its pores when placed in oil, displacing water (Crain, 2006). Spontaneous imbibition is

mainly affected by capillary forces, and is driven by surface energy and capillary pressure difference across the interface between two immiscible fluids.

Spontaneous imbibition experiments can also help determine the relative permeability characteristics of the rock, and so imbibition tests were conducted using oil and water on clean cores, as well as cores exposed to crude to test wettability alteration in the cores. The weight gain was measured with time, and the recovery was calculated using the following:

$$Recovery = \frac{Wt. \text{ with wire in fluid}_{current} - Wt. \text{ with wire in fluid}_{initial}}{\rho_{fluid, displacing} - \rho_{fluid, displaced}} * \frac{1}{PV} \quad (10)$$

Where,

$\rho_{fluid, displacing}$: Density of the displacing fluid, either oil or water, in gm/cm³

$\rho_{fluid, displaced}$: Density of the displaced fluid, either oil or water, in gm/cm³

$Wt.$: Weight, in gm

PV : Pore volume, in cm³

However, to calculate the recovery fraction, the initial weight of the wire in fluid at T_{zero} is very important, and it is very difficult to obtain it without errors. For this purpose, this weight is back calculated using the buoyancy force exerted by the liquid.

$$Wt. \text{ with wire in fluid}_{initial} = Wt. \text{ with wire in air}_{initial} - F_{buoyancy} \quad (11)$$

There are two methods to calculate the buoyancy force, through the weights, and though the rock volume.

$$F_{buoyancy} = Wt. \text{ with wire in air}_{final} - Wt. \text{ with wire in fluid}_{final} \quad (12)$$

$$F_{buoyancy} = V_{rock} * \rho_{fluid} \quad (13)$$

Where,

Wt. is measured in grams,

V_{rock} : Rock volume, in cm^3

ρ_{fluid} : Density of the fluid, in gm/cm^3

The final saturation of the rock following imbibition is then calculated using the following equation:

$$Saturation_{final} = \frac{Wt. \ no \ wire_{final} - Wt. \ no \ wire_{initial}}{\rho_{fluid,displacing} - \rho_{fluid,displaced}} * \frac{1}{PV} \quad (14)$$

3.5 Relative Permeability

Since the recovery of formation fluids depends on the wettability of the rock, relative permeability data is required to quantify this wettability. Relative permeability is defined as the ratio of the effective permeability of a fluid to the absolute permeability of the rock, when the fluid occupies just a fraction of the total pore volume. A typical example of this relationship is shown in **Figure 15**. Relative permeability is also dependent on the saturation and distribution of the fluids (Honarpour & Mahmood, 1988), and it helps to understand the wettability characteristics of the rock when it is subjected to two-phase flow with two or more immiscible fluids. This data is essential for almost all calculations of fluid flow in hydrocarbon reservoirs, and can help make estimates of productivity, injectivity, ultimate recovery as well as for diagnosis of formation damage expected under various operational conditions (Honarpour & Mahmood, 1988).

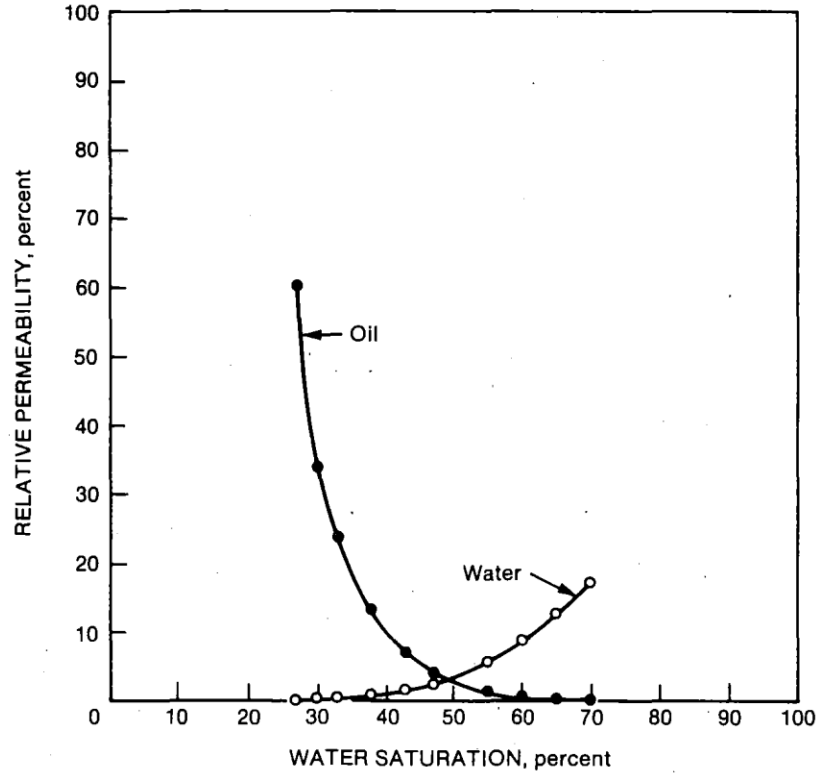


Figure 15: Typical Water/Oil relative permeability curve (Honarpour & Mahmood, 1988)

Since relative permeability describes the simultaneous flow of more than one fluid, it is necessary to generalize Darcy's law, using the concept of effective permeability. Effective permeability can be described as the permeability of a rock to a particular fluid, when more than one fluid is present in the reservoir. When only one fluid is present in the formation, the absolute and effective permeabilities would be equal. Effective permeability can be calculated by:

$$k_{eo} = \frac{q_o \mu_o L}{A \Delta P_o} \quad (15)$$

$$k_{ew} = \frac{q_w \mu_w L}{A \Delta P_w} \quad (16)$$

Where,

q_o, q_w : flow rate of oil and water at the specific saturations, in cm^3/sec

μ_o, μ_w : viscosity of oil and water, in centipoise (cp.)

$\Delta P_o, \Delta P_w$: Pressure drop for each phase – oil and water at specific saturations, in atm.

k_{eo}, k_{ew} : Effective permeability to oil and water, at specific saturations, in Darcy (D)

Using these, relative permeability can be defined as:

$$k_{ro} = \frac{k_{eo}}{k} \quad (17)$$

$$k_{rw} = \frac{k_{ew}}{k} \quad (18)$$

Where,

k : absolute permeability, in D

k_{eo}, k_{ew} : Effective permeability to oil and water, at specific saturations, in D

k_{ro}, k_{rw} : Relative permeability to oil and water, at specific saturations

The value of relative permeability is fractional and dimensionless, and is reported in decimal form. Relative permeability can be zero, if there is no flow, as in case of irreducible fluid saturation. The value of relative permeability is dependent on the specific saturation, and varies as the saturation of the fluids in the pore spaces change. Various methods to calculate the saturation of the fluids in the core exist, but in this case, for a two-phase system, the saturation is calculated by:

$$S_w = \frac{V_w}{V_p} = \frac{W_{sat} - W_{dry} - \rho_o V_p}{\rho_w - \rho_o} * \frac{1}{V_p} \quad (19)$$

$$S_o = 1 - S_w \quad (20)$$

Where,

S_w, S_o : Water and oil saturations

W_{sat} : Saturated weight of the core, at a particular flow rate, in grams

W_{dry} : Initial dry weight of the core, in grams

ρ_o, ρ_w : Density of oil and water, in gm/cm^3

V_p : Pore volume, in cm^3

CHAPTER 4: EXPERIMENTAL DESIGN AND METHODOLOGY

4.1 Objective

Since asphaltene precipitation, deposition and the resulting alteration of rock characteristics is a well-documented problem, work done in the research for this thesis focused on recreating the deposition effects and problems typically encountered in the field. Based on the experiences of other research groups, our study focused on addressing several shortcomings to create more realistic samples which could be tested in the lab for the problems caused by asphaltene precipitation. The first step in this process was to properly characterize the crude and core samples, followed by determining a suitable method to develop a uniform deposition profile in those core samples. Once this is achieved, the effect of this deposition on rock characteristics could be effectively studied and modeled to reservoir scale.

4.2 Experimental Workflow

To evaluate the impact of asphaltene precipitation, and the ensuing wettability changes, experiments were conducted to first create a uniform deposition of asphaltene in core samples, followed by measuring and quantifying the impact of this precipitation and deposition on rock characteristics and finally studying the impact of the changes in the rock characteristics on a field model. The experimental process which was followed started by selecting a suitable crude oil, measuring the asphaltene content of the crude oil, ensuring that this crude caused precipitation of asphaltene in the core samples, determining the best saturation method to get uniformity in asphaltene deposition, measuring the porosity and changes in permeability of the cores, ensuring the uniformity of the deposition in the core samples, followed by determining the wettability changes

through imbibition tests as well as liquid permeability measurements. These results were then compared to a base case, and modeled to determine the impact on ultimate recovery on a field scale.

4.3 Equipment and Materials

4.3.1 Rocks

The rocks used for the study were Grey Berea sandstones purchased from Kocurek Industries. Grey Berea samples are easily available, have good porosity and permeability, and are ideally suited to study the impact of asphaltene deposition on sandstone rock characteristics. Samples of 2 inches and 6 inches in length and 1 inch in diameter were cored from the rock. Water was not used in the coring process as the rocks were prone to clay swelling, and so the coring process was done with a diamond tipped bit, while using air as a medium to circulate out the cuttings. The cored samples were also polished to achieve a flat surface.

4.3.2 Fluids and Gases

The crude used for the study was generic Texas crude obtained from a field in Midland, Texas. Texas crude was used for the experiments since it was easily available, and had a reasonable amount of asphaltene present in the crude. Care was taken to ensure that the crude used was from a single batch to avoid significant changes in the asphaltene content. The crude was characterized by measuring its density and viscosity, as well as by determining its asphaltene content.

Brine was used for the study as the rocks used in the study were found to be prone to clay swelling when exposed to fresh water. 3% by weight concentration brine was prepared by mixing common salt (Sodium Chloride, NaCl) with deionized water. 3% brine was used since reservoir water typically has a similar salt concentration. This brine was used in imbibition, injection as well as relative permeability tests.

The chemicals used for the study were purchased from Sigma Aldrich. These chemicals included heptane, toluene and acetone. Heptane was used as the liquid which displaces the crude oil from the cores, as it does not dissolve the asphaltenes. Toluene was used mainly for the cleaning of the setup, during the asphaltene content filtration test, as well as to remove the asphaltene deposition. Acetone was used mainly for the cleaning of the equipment. Helium and nitrogen was used to measure the porosity and permeability respectively.

Table 1: Fluids used in the experiments, and their properties (at 20°C)

Fluid & Gases	Density (gm/cm³)	Viscosity (cp.)	API Gravity	Concentration
Texas Crude	0.884	19	27	-
Brine	1.021	1.32	7.1	3% by weight
Heptane	0.684	0.376	71	99%
Toluene	0.865	0.560	32	99%
Deionized Water	1	1	10	-
Helium	0.000178	0.0196	-	-
Nitrogen	0.00125	0.0178	-	-

4.3.3 *Equipment*

The equipment used for the experiments conducted in this study were either developed in house such as the porosimeter, or purchased such as the Hassler type core holder, the ISCO pumps from Teledyne, accumulators, pressure transducers, fittings from Swagelok, a CentriVap Cold Trap as well as a Mettler Toledo weighing machine. The porosimeter and the core holder were both designed for 1-inch diameter cores, and so all the tests were done using cores of this size. The porosimeter could hold samples ranging from 0.1-6 inch in length, while the core holder could accommodate samples up to 12 inches in length. The filter paper used for testing the asphaltene content was a Grade 5 Filter Paper from Watson which had a pore size of about 2.5 μm , and a slow flow rate, which was required for the filtration test.

4.4 Characterizing the Crude and Deposition Potential

4.4.1 *Measuring Asphaltene Content*

Texas crude used for this study typically has not been used for asphaltene studies, given that it is lighter in nature, and thereby has a potential for a lower asphaltene concentration. Given the limitations in obtaining a heavier crude for the study, the initial objective of the study was to measure and ensure that there was asphaltene particles present in the crude and quantify it. A modified form of the ASTM IP143 Standard for the Determination of Asphaltenes in Crude Petroleum was used, which was also employed by Goual and Firoozabadi in their research (Goual & Firoozabadi, 2004). The equipment used for this consists of a filtration flask and funnel connected to a vacuum pump through plastic tubing's. Asphaltenes are filtered using a Whatman Grade 5 filter

paper (90 mm diameter and 2.5 μm pore size). The weight is then measured using a Mettler Toledo analytical balance which has an accuracy of 0.001 g.

The process starts with Texas crude being mixed with heptane at a weight fluid ratio of 1:40 g/ml. About 5 gm of crude was mixed with 200 ml of heptane in this experiment. The mixture is then left for about 24 hours to age, after which the mixture is filtered using the conical flask and the vacuum setup. The filter paper is placed at the top of the conical flask after weighing it, and vacuum is applied from the side of the conical flask. This is shown in **Figure 16**. Asphaltene particles which are larger than the pores of the filter paper are retained on it. The filter paper is then washed with heptane again before being left to dry. Once the solvent has evaporated, the filter paper is weighed again, and the difference is used to calculate the weight % of asphaltenes in the crude.



Figure 16: Asphaltene content measurement setup. The filter paper is placed on top of the conical flask.

4.4.2 *Deposition Potential*

Once the asphaltene content in the crude has been measured, the next step was to ensure that this crude induces asphaltene precipitation and drop out. This was done by a

simple bottle test, during which the Texas crude was mixed with Heptane in a 1:2 and 1:4 ratio. 2 gm of crude was mixed with 4 gm of heptane in the first case, and with 8 gm of heptane in the second case. The bottles were agitated and then allowed to rest for 24 hours, as shown in **Figure 17**.

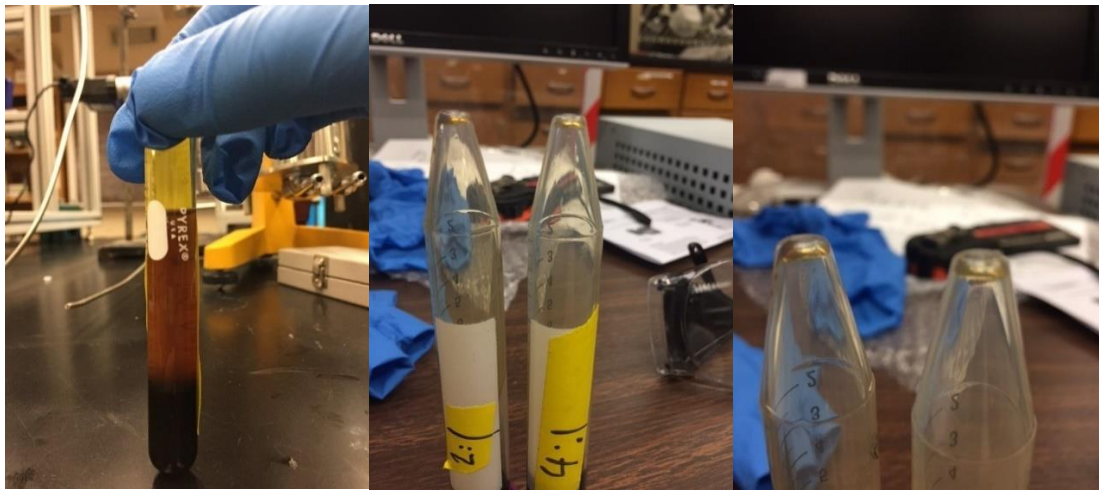


Figure 17: Bottle tests with heptane and crude mixed in 2:1 and 4:1 ratios to determine the asphaltene precipitation potential.

The next step was to evaluate if dropout occurs when the crude is passed through a core sample. This was done by injecting the crude through a core sample, and monitoring the pressure drop across the sample. An increasing pressure would be an indication that there was precipitation and possible deposition/blocking of High Molecular Weight components (HMW) in the core sample, which could be asphaltenes, waxes or resins.

This was done by using a Hassler type core holder which has a rubber sleeve inside to hold the dry core sample. The inlet line was attached to a pressure transducer, and an accumulator containing crude oil. The accumulator was in turn attached to an ISCO pump, which moves the piston inside the accumulator to pump the crude oil into the core

holder. The outlet line of the core holder was open to the atmosphere, and the fluid coming out was collected in a beaker. Pressure was monitored continuously, and plotted as a function of time to determine possible precipitation and blockage.

4.5 Rock Preparation

Once the cores were cut and polished, the physical properties such as the length and diameter were measured and averaged at 5 points to have accurate dimensions. The dry weight of the core was also noted as it is required for saturation calculations.

4.5.1 Porosity

To measure the porosity of the rocks, a porosimeter which was designed in-house was used. The porosimeter contained 7 spacers measuring 2.5-inch, 1.5-inch, 1-inch, 0.5-inch, 0.25-inch, 0.15-inch and 0.1 inch in length (labeled 1-7) to account for different core sizes. The pressure transducer used was by Swagelok and having a 0-300 psi range. The schematic for the porosimeter is shown in **Figure 18**.

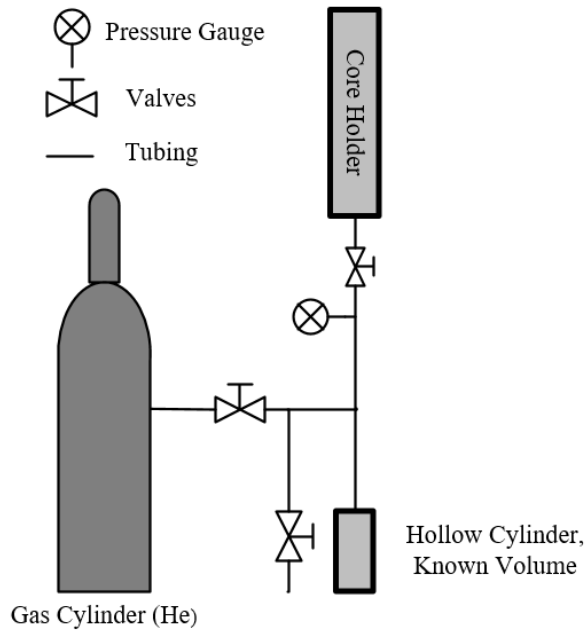


Figure 18: Porosimeter used in the study. The core is placed in the chamber at the top.

The porosimeter was calibrated using the solid spacers, and using Boyle’s law as described earlier. An excel sheet was prepared to be more user friendly, and which would require only the length, diameter, weight, the pressure readings before and after opening the valves and the spacers inside the porosimeter to calculate the porosity, bulk and matrix density and the pore volume. The steps for measuring porosity are as follows:

1. Length, diameter and weight of sample measured, and input in the excel sheet.
2. Spacers removed from the porosimeter, and a combination of spacers about the same length as the core sample is selected.
3. The remaining spacers, along with the core sample is now placed inside the porosimeter, and the end-cap is tightly shut.

4. The porosimeter is then charged with helium up to 200 psi pressure, while making sure that the relief valve, and the valve leading the core holder are shut.
5. The helium supply valve is then shut, and pressure is allowed to stabilize. Initial pressure P1 is measured.
6. Now the valve connecting to the core holder is opened, and the pressure P2 is noted from the gauge.
7. Pressure is then released from the porosimeter using the relief valve. Core sample is unloaded, and spacers replaced in the system.
8. The data is entered in the excel sheet to calculate the porosity.

4.5.2 *Permeability*

Once the porosity was measured, the gas permeability of the cores was measured using a Hassler type core holder. Core samples were placed in a rubber sleeve inside the core holder, and since the core holder can take cores up to 12 inches in length, a series of spacers was used. The spacers had holes through the center to allow the fluid to flow. A confining pressure of 1500 psi was applied around the core and spacers using the rubber sleeve. The schematic of the permeability setup is shown in **Figure 19**.

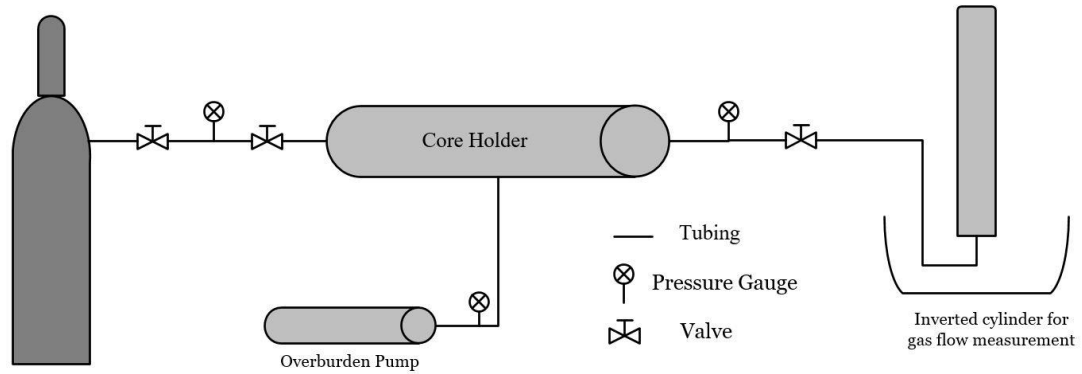


Figure 19: Schematic of the setup to measure gas permeability of the core samples.

Nitrogen gas was flown through the system, and Swagelok pressure transducers (of 0-300 psi range) placed at the inlet and the outlet of the core holder was used to measure the pressure drop across the system. An overburden pump, attached to a high-pressure gauge (0-2000 psi range) was used to apply the overburden pressure around the core sample. Permeability measurements were taken both in the presence of a back-pressure regulator, and without it, during which the outlet would be open to atmospheric pressure. The flow rate was measured manually using an inverted graduated cylinder filled with water, and a stop watch. Another excel template was prepared for calculating permeability using both Darcy and Forchheimer equations. The steps for measuring permeability are:

1. The outlet cap on the left of the core holder is unscrewed, and the spacers are removed from the core holder.
2. The core was loaded into the core holder so that it is in contact with the inlet. Spacers were replaced into the core holder, leaving behind a combination of spacers about the same length as the core.

3. The end cap was screwed back on the core holder, and the adjustable screw was tightened to make sure that the core and the spacers are tightly held between the end caps.
4. A confining pressure of about 1500 psi was applied using the confining pump.
5. The outlet line was attached to a pressure gauge, a back-pressure regulator and a flexible plastic line was connected to this to take the volume readings using the graduated cylinder.
6. The inlet line from the core holder was connected to another pressure gauge, and the nitrogen gas tank.
7. The tank was then opened, and nitrogen was flowed through the core holder. Inlet pressure was maintained at around 100 psi.
8. Using the back-pressure regulator, the outlet pressure was then set to 50 psi.
9. An inverted graduated cylinder filled with water was placed in a bowl containing water, and the initial volume was recorded.
10. Once pressures stabilized, nitrogen from the outlet was introduced into the inverted cylinder using the plastic line and timed using a stopwatch. The inlet pressure, outlet pressure, final volume in the cylinder and the time taken to displace the water in the cylinder is noted.
11. This is then repeated for 5psi increments of outlet pressure using the back-pressure regulator and the new pressures and volumes are noted.
12. Once the required number of readings were obtained, the nitrogen tank is shut, and the confining pressure is released.
13. The core is unloaded from the core holder, and the spacers were replaced back.

14. In the absence of a back-pressure regulator, the same process is used except that the outlet line is completely unregulated, and the inlet pressure is changed in 5 psi increments to get pressure and volume data.
15. The data collected is entered in the excel sheet to calculate the permeability.

4.6 Uniformity of Deposition

Once the properties of the core sample were measured, and since it was established that the crude does indeed cause asphaltene precipitation in the rock, the next step was to determine a method which would ensure that the deposition of asphaltene would be nearly uniform throughout the core sample. Two different methods were used to induce asphaltene precipitation in the rock, simple injection of crude and vacuum saturation of the cores. The uniformity was then evaluated using permeability measurements of representative sample sizes, as well as through Total Organic Carbon (TOC) analysis.

4.6.1 Injection

The first method used to saturate the core samples with crude, and to induce precipitation of asphaltene was by simple injection of Texas crude into the core samples. Berea cores of 2 inches in size were used for this, and the experiment was conducted in a smaller Hassler type core holder as shown in **Figure 20**. The core holder could take cores of up to 3 inches in length, 1 inch in diameter, and has a pressure transducer attached to the inlet to measure the injection pressure. Two accumulators, one for crude and one for heptane, which are connected to ISCO pumps are used for the injection process. The core

was aged for a period ranging from 2 weeks to 3 months following this. The process followed is below:

1. The properties of the core including length, diameter, weight, as well as the porosity and permeability are measured.
2. The bottom end cap of the core holder was opened, and the core was loaded into the core holder. The bottom endcap is then screwed close, while ensuring the core is in contact with the top end cap, which is adjustable.
3. The crude accumulator is connected to the ISCO pump, and the valves connecting the heptane accumulator to the core holder is shut.
4. The line connecting the crude accumulator to the core holder is then primed with crude by using the ISCO pumps, to remove any air in the system.
5. The line is then attached to the endcap of the core holder, and the initial pressure is noted.
6. A confining pressure of 1500 psi is then applied around the core using the confining pump, and the valves connected to this pump are closed.
7. The ISCO pumps are then run at a rate of 2 cc/min, so that crude flows through the core at this rate.
8. Crude is flowed through the core for about 30 minutes, or 6 pore volumes (PV), and pressure is continuously noted to ensure that there is deposition.
9. Following this, the pumps are stopped, and the pressured is allowed to drop. The confining pressure valves are opened to remove confining pressure around the core.

10. The end cap is opened, and the core is removed, weighed, and placed in a sample of crude to age.
11. An additional process was also conducted on certain cores in which heptane and crude was co-injected into the core. Slug injection of heptane followed by crude injection was also done on certain cores, before they were fully saturated with crude.

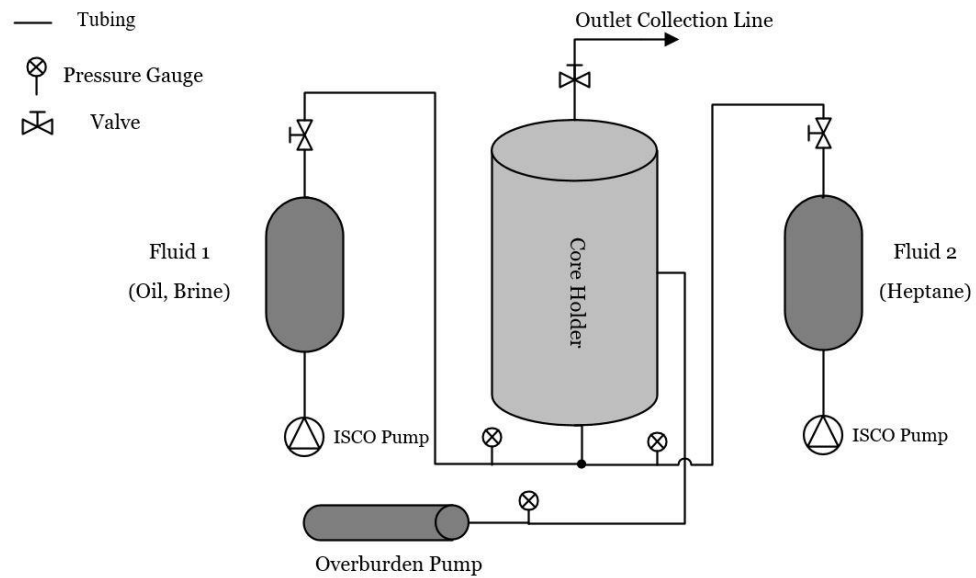


Figure 20: Hassler sleeve core holder used for injection tests (for cores up to 3-inches in length)

4.6.2 Vacuum Saturation

The second method used to induce precipitation of asphaltene in the core was by vacuum saturating the core sample with crude oil. The schematic for the saturation setup is shown in **Figure 21**. It basically consists of a conical saturation flask, which is connected to a vacuum pump through a series of valves, a pressure gauge and a cold trap. The CentriVap Cold Trap, which operates at around -105°C is used for the process to

ensure that fluids from the saturation setup do not enter the vacuum pump, which could ruin the equipment. The process followed for the saturation of the sample is as follows:

1. The cold trap is turned on for 1-2 hours before the experiment is started. Ensure that the connections between the vacuum pump, cold trap and the valves are tight and leak proof.
2. Side load the core in the clean and dry conical saturation flask and slowly turn it up right to avoid any damage to the core or to the flask.
3. Place the rubber stopper on top of the saturation flask, to seal the top. Be careful to avoid leaks in the system.
4. The plastic tube attached to the valve system is then connected to the neck of the saturation flask, and the clamping is tightened around the neck. The valves connecting the flask to the cold trap and the vacuum pump are then opened.
5. A large beaker is filled with about 2 liters of the saturating fluid (crude), and the saturating fluid inlet line is placed in the beaker. Make sure that the valve connected to the saturating fluid inlet line is closed at this point.
6. Now switch on the vacuum pump, and then quickly open and close the valve connected to the saturating fluid inlet line so that the line could be primed with the saturating fluid (crude).
7. Vacuum the setup for about 2 hours, and periodically check if the vacuum is working properly by making sure that the pressure gauge shows a pressure of about -25 psi.

8. No close all the valves connecting the conical saturation flask to the vacuum pump and the cold trap. Open the valve connected to the saturating fluid inlet line so that the saturating fluid can fill the conical flask which is under vacuum.
9. When the core is fully submerged, close the saturating fluid inlet line.
10. Turn off the vacuum pump and the cold trap at this stage and allow the submerged core to sit for 24 hours under vacuum.
11. Once the core has been saturated for 24 hours, disassemble the conical saturation flask, and transfer the core to a beaker containing the saturating fluid to further age for 2 weeks to 3 months.
12. Disassemble the valves and clean the entire setup with toluene and acetone to prepare for the next use.

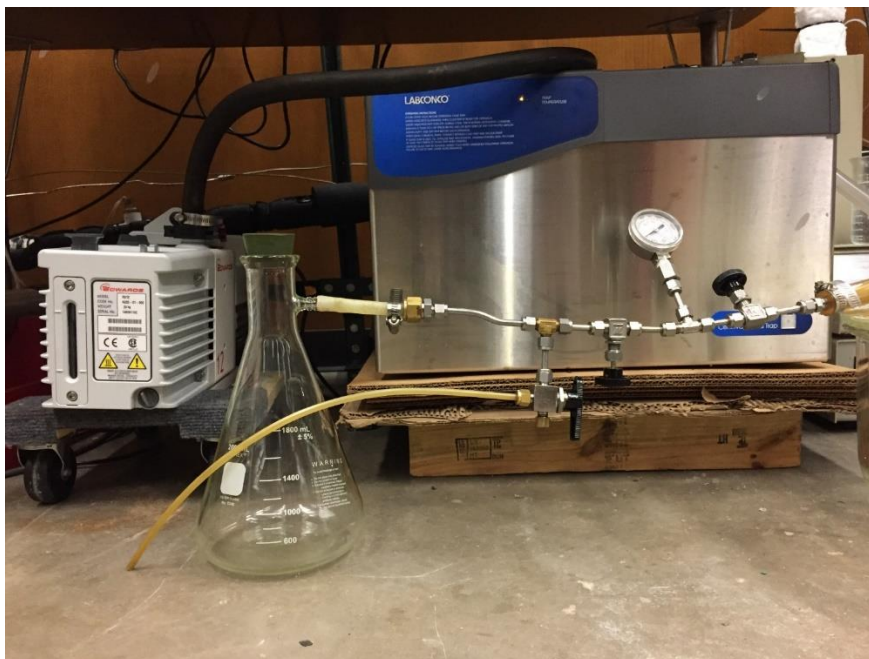


Figure 21: Vacuum saturation setup. The cores are placed in the conical flask, and the vacuum pump is connected to the flask through a cold trap.

4.6.3 *Evaluating by Density, Permeability and Sample Sizes*

To evaluate the uniformity of deposition, the cores saturated with crude through the injection process and the vacuum saturation process were both first flushed with heptane for 4 pore volumes (PV) to remove the crude. This would also ensure that all crude components including the high molecular weight components such as paraffin's and waxes would be washed away, but leaving behind the asphaltenes deposited on the surface, since asphaltenes are not soluble in heptane. The setup used for this process was the same injection setup, but the accumulators were replaced with heptane. Since the cores were saturated with crude, care was also taken not to introduce any air into the system, and the cores. This was followed by drying the cores in an oven at 100°C for 24 hours, followed by a cooling period of about 2 hours.

Once the impacted cores are cooled, permeability was measured using the longer, hassler type core holder, but without using the back-pressure regulator. Nitrogen gas was again used as the fluid medium for the measurements. The cores were then cut into two half pieces, and permeability was again measured for uniformity. Results are noted, and the half pieces were again cut to quarter pieces, and permeability was measured again. The steps for this are described below:

1. The cores containing crude from both the injection process and the vacuum saturation process are weighed.
2. The impacted core was loaded into the small core holder and the bottom endcap is then screwed close. The top end cap is adjusted to make sure that it is in contact with the core.

3. The accumulator containing heptane is connected to the ISCO pump, and the line is then primed with heptane, to remove any air in the system.
4. The line is then attached to the endcap of the core holder, and the initial pressure is noted.
5. A confining pressure of 1500 psi is then applied around the core using the confining pump, and the valves connected to this pump are closed.
6. The ISCO pumps are then run at a rate of 2 cc/min and pressure is continuously noted. The pumps are stopped when the fluid coming out of the outlet line is clear, without any hint of crude.
7. Following this, the core is removed, weighed, and placed in an oven for 24 hours so that the heptane could evaporate.
8. After this, the impacted core is removed, and allowed to cool for about 2 hours.
9. Weight is measured after this period, and the weight and density change are calculated.
10. Following this, the core is loaded into the core holder along with spacers. The end cap is screwed back on the core holder, and the adjustable screw is tightened to make sure that the core and the spacers are tightly held between the end caps.
11. A confining pressure of about 1500 psi was applied using the confining pump.
12. The inlet line from the core holder was connected to a pressure gauge, and the nitrogen gas tank, while the outlet line was open to the atmospheric pressure.
13. Nitrogen is flowed through the core holder, and the inlet pressure is set to 5 psi.
14. An inverted graduated cylinder filled with water was placed in a bowl containing water, and the initial volume was recorded.

15. Once pressures stabilized, nitrogen from the outlet was introduced into the inverted cylinder using the plastic line and timed using a stopwatch. The inlet pressure, outlet pressure, final volume in the cylinder and the time taken to displace the water in the cylinder is noted.
16. This is then repeated for 5 psi increments of inlet pressure and the new pressures and volumes are noted.
17. Once the required number of readings were obtained, the nitrogen tank is shut, and the confining pressure is released.
18. The core is unloaded from the core holder, and was cut into half pieces. The process from steps 9-17 is repeated. This was followed by again cutting the core into quarter pieces, and repeating steps 9-17.

4.6.4 Evaluating by TOC

An additional method to evaluate the uniformity of deposition was by measuring the total organic carbon (TOC) content in the impacted core. For this, the saturated cores from the injection process, and the crude saturation process are first flushed with heptane to remove the crude, and any HHW components except asphaltenes. This was followed by taking representative samples from three areas of the impacted core; one from the inlet, once from the outlet, and one from the center. These three samples from each core is analyzed for carbon content to determine the level of deposition. A sample which was not exposed to crude was also used as control. The steps followed for this test is as follows:

1. The impacted cores containing crude from both the injection process and the vacuum saturation process are weighed.

2. Steps 2-9 from the previous process is repeated to remove any heptane soluble crude component from the impacted core.
3. The impacted rocks are cut in such a way that a small sample is obtained from the inlet, outlet, and the center. Three samples are also obtained from a clean rock by the same process.
4. These samples are then crushed into fine particles, and is properly labelled for the TOC measurement.
5. TOC values are reported as fractions.

4.7 Evaluating Wettability Alteration

Once the uniformity of deposition is evaluated, the next step was to evaluate how the deposition of asphaltenes affect the rocks. The exposed cores were aged for different periods before wettability alteration tests were done. This was because asphaltene molecules are polar, and the adsorption or deposition of the molecules to the pore surfaces stabilizes with time. Wettability alteration was then quantified and evaluated through pressure drop tests across the cores, as well as through imbibition tests. The tests were also done on clean cores to obtain a baseline for the results, and determine how the properties are altered.

4.7.1 Evaluating Pressure Drop Through Core flooding

Pressure drop tests were done on all core samples which were exposed to crude, and as a result, potentially impacted with asphaltene precipitation. Three primary scenarios were used: The first scenario was in which the samples were initially saturated

with crude, and then flushed with heptane, dried, and then injected with brine followed by heptane. The second scenario was a clean sample which was injected with brine, followed by heptane, and the third scenario was in which the samples were injected with brine, saturated with crude, followed by a flush with heptane, dried and then injection with brine followed by heptane. This was done to achieve different primary wetting phases in the cores and see how they reacted with asphaltene precipitation and deposition.

The setup used for this process was the same smaller hassler type core holder, and it was connected to a brine, heptane and crude accumulator, which were operated through ISCO pumps. Pressure was continuously monitored throughout each of these injection processes. The steps followed are listed below:

1. The properties of the cores such as length, diameter, weight, porosity and permeability are measured. In case the core was saturated, the crude in the core was washed away with heptane, dried and permeability was measured again without back pressure.
2. The bottom end cap of the core holder was opened, and the core was loaded into the core holder. The bottom endcap is then screwed close, while ensuring the core is in contact with the top end cap, which is adjustable.
3. The brine accumulator is connected to the ISCO pump, and the valves connecting the heptane accumulator to the core holder is shut.
4. The line connecting the brine accumulator to the core holder is then primed to remove any air in the system and then attached to the endcap of the core holder.
5. A confining pressure of 1500 psi is then applied around the core using the confining pump, and the valves connected to this pump are closed.

6. The ISCO pumps are then run at a rate of 2 cc/min, so that brine flows through the core at this rate. The flow was continued till the pressures stabilized, which took about 60-70 minutes. The pressures with time is noted.
7. Following this, the pumps are stopped, and the pressured is allowed to drop. The confining pressure valves are opened to remove confining pressure around the core.
8. The end cap is opened, and the core is removed, weighed, and then loaded back into the core holder.
9. The valve connecting to the heptane accumulator is then opened, while the valve to the brine accumulator is closed. The line is then primed with heptane, and is connected to the end cap.
10. Confining pressure is 1500 psi is again applied around the core, and the pump is run at a rate of 2 cc/min. The flow is again continued till the pressure stabilized, which took around 15-20 minutes.
11. The pressures are noted again, and the volume of brine displaced by the heptane is collected.
12. Following this, the pumps are stopped, confining pressure is released, and the core is removed and weighed.
13. The steps are repeated for the next core samples, as well as for reproducibility.
14. The pressures are plotted and compared for the different cores.

4.7.2 Imbibition Tests

Wettability change was also evaluated using imbibition tests, which were conducted on a clean rock (as control) and an impacted rock (which was saturated with crude and cleaned and dried with heptane) (Mehana, Al Salman , & Fahes, The Impact of Salinity on Water Dynamics, Hydrocarbon Recovery and Formation Softening in Shale: Experimental Study, 2017). Water and Heptane were both used for the imbibition tests, and the behavior of the rock towards each of these fluids was noted.

The imbibition setup mainly consists of the Mettler Toledo balance, which has an accuracy of $\pm 0.001\text{g}$. The balance was placed on a stand, with a hole at the bottom, through which a line connected to a fish hook was attached to the bottom of the balance. This is shown in **Figure 22**. The core samples were then suspended from the hook, into the displacing fluid, and weight was recorded continuously on a computer. The process followed for measuring the imbibition data is as follows:

1. The impacted core, or a clean core which is at room temperature is used.
2. The properties of the core are measured including the length, diameter, weight, porosity and permeability. Pore volume is calculated from this data.
3. Densities of the imbibition fluids (Water/brine, heptane) at room temperature is noted.
4. A string is tied around the sample securely and the weight of the sample in air, with the string attached is measured.
5. The sample is then suspended from the fish hook connected to the balance using the string.

6. The software to monitor the weight is loaded on the computer, and make sure that the weight is recorded continuously at three second intervals on an excel sheet.
7. Now, using a stopwatch in one hand, the sample was carefully dropped into a beaker filled with the imbibing fluid (either water/brine or heptane). The stopwatch was simultaneously started to obtain a correct starting time for the experiment, which could be compared to the data from the computer.
8. Spontaneous imbibition is allowed to continue for 14-24 hours to ensure that the core saturation reached equilibrium and that there was no weight change in the core sample at the end of the experiment.
9. The final weight of the core suspended in the fluid at the end of the imbibition was noted.
10. The core is then removed from the fluid and excess liquid on the surface is cleared. The core with the string is then weighed again, and this is noted as the final weight of the core with string attached in air.
11. The string is then removed, and the core sample is weighed again, and noted as the final weight of core in air. An excel spreadsheet is then used to calculate recovery.
12. The sample is then placed in an oven at 100°C for 24 hours, followed by a cooling period of about 2 hours, so that the imbibed fluid evaporates, and the test could be done again with another fluid.

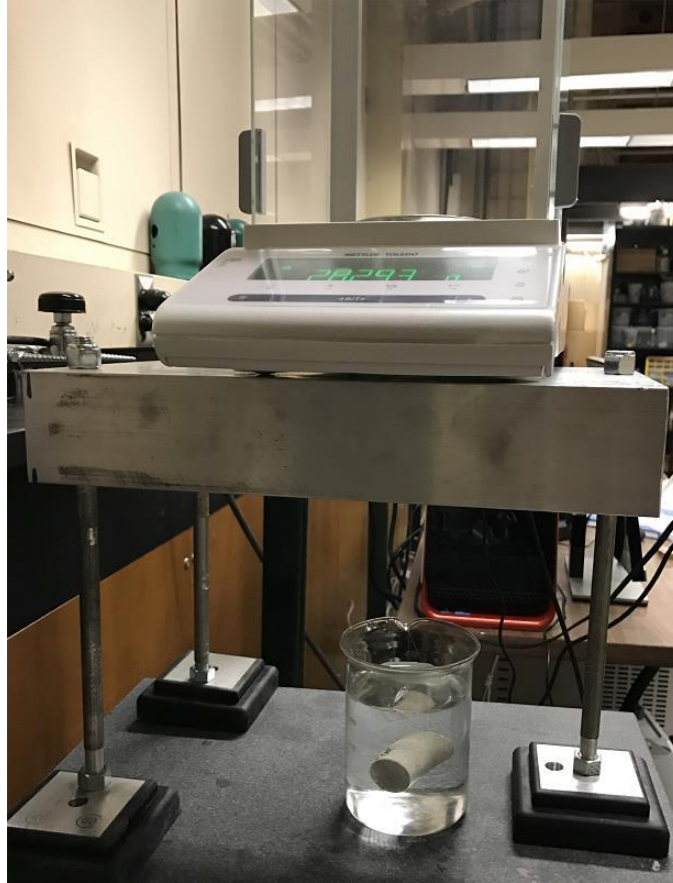


Figure 22: Imbibition setup which consists of a Mettler Toledo balance, from which the core sample is suspended in the fluid.

4.8 Relative Permeability Tests

Relative permeability tests were conducted to evaluate the extent of the wettability change, the data of which could be used in a reservoir simulation. The test was conducted using 6-inch-long cores – an impacted core which had been saturated with crude and flushed with heptane, as well as a clean core, as control. The longer hassler type core holder, along with two accumulators, and two ISCO pumps was used for this experiment. The setup is shown in **Figure 23**. Brine and heptane was injected with various ratios to obtain the relative permeability curves. Additional points for the relative permeability curves were obtained using Corey’s correlations. The procedure is explained below.

1. The impacted core which has been flushed with heptane to remove the crude, and dried is used for measuring the changed relative permeability. A clean core is used to obtain the base case relative permeability.
2. The properties of the core are measured including the length, diameter, weight, porosity and permeability.
3. Following this, the core is loaded into the long core holder along with spacers in such a way that the core is in contact with the inlet line. The end cap is screwed back on the core holder, and the adjustable screw is tightened to make sure that the core and the spacers are tightly held between the end caps.
4. A confining pressure of about 1500 psi was applied using the confining pump.
5. A system of valves which open to the brine accumulator or the heptane accumulator is used to control the flow. The accumulators are attached to two separate ISCO pumps. The valve connected to the brine accumulator is opened first, while the heptane valve is closed.
6. The lines connecting the accumulators to the core holder are primed with brine, and then connected to the end cap of the core holder.
7. Brine is then injected into the core at a rate of 1 or 2 cc/min for several pore volumes to fully saturate the core. Pressure is continuously monitored at this stage.
8. Following this, the pump is stopped, lines are disconnected, and the confining pressure is removed. The core is removed from the core holder and weighed.
9. The brine valve is then closed, and the heptane valve is opened. The line, as well as the inlet end cap is primed with heptane to avoid any air in the system.

10. The core is then placed into the core holder again, but pressed against the inlet end cap to avoid any air entering the core. The end cap is tightened, and the lines are connected.
11. Confining pressure of 1500 psi is applied on the system.
12. Heptane is then injected into the core at a rate of 1 or 2 ccc/min for several pore volumes to achieve irreducible water saturation. The volume of brine coming from the outlet is collected and noted.
13. Pressure is again continuously measured for this stage. After the pressure stabilizes, the outlet volumes are measured to ensure that the inflow and outflow has stabilized.
14. Once steady state is achieved, flow is stopped, and the core is again removed from the core holder and weighed.
15. Following this, both the heptane and brine valves are opened. The lines and the end cap are primed to remove any air, and the core is carefully placed in the core holder again. Confining pressure is applied again on the core.
16. The steps are then repeated, and heptane and brine are co-injected into the core at varying ratio's. The core is removed from the core holder and weighed at the end of each injection rate, once study state is achieved.
17. The weights are used to calculate the saturations, while the injection rates and the end pressures are used to calculate the relative permeabilities.
18. This data is then plotted to obtain the relative permeability curves.

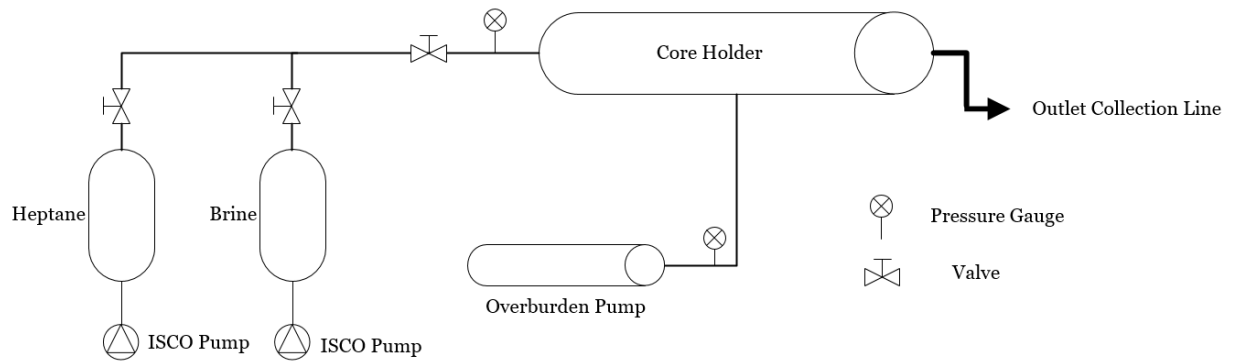


Figure 23: Schematic of the brine-heptane relative permeability setup

4.9 CMG Modeling

To quantify the impact of the wettability change, and the shift in the relative permeability end points, a CMG simulation model of a field undergoing water flood was adopted. CMG IMEX simulator (Black oil) is used. Relative permeability data obtained from the relative permeability experiment on the impacted cores was used for the evaluating the results.

The reservoir is modeled with a 50x35x20 heterogeneous cartesian grid, which has about 35000 grid blocks. The field has a total of 11 wells, two of which are initially producing and later converted to injectors. Depth of the reservoir was around 6800 ft. and an infinite acting aquifer provided the boundary support below the reservoir for pressure maintenance. The pay zone thickness was about 37 meters, and the oil-water contact was at 5740 ft. The grid is shown in **Figure 24**.

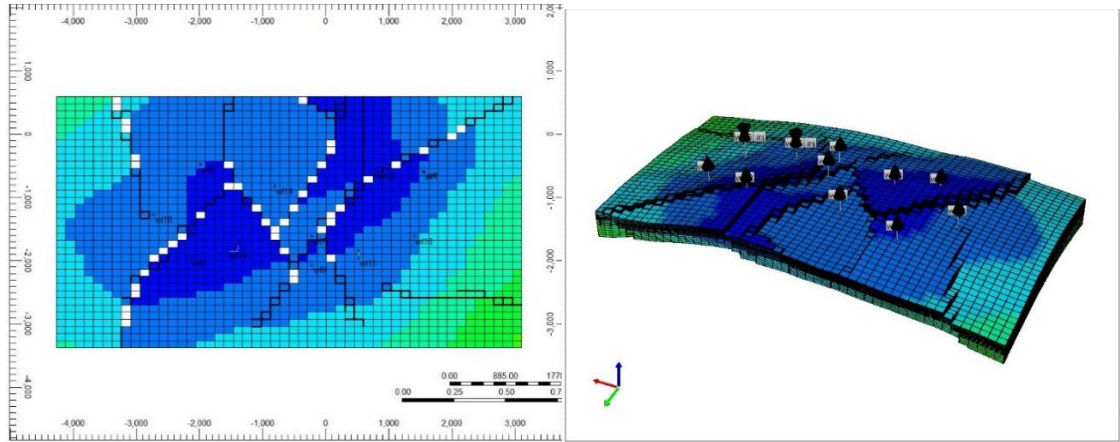


Figure 24: The reservoir top view (left) and side view (right)

The reservoir had an average permeability ranging from 30-300 md, and a porosity ranging from 8-25%. The reservoir temperature is 122F, and the fluid properties were specified for the reservoir, as per **Table 2**. The permeability and porosity maps of the field grid tops are shown in **Figure 25**. The relative permeability data was calculated from the built-in correlations in CMG using the end points estimated from the relative permeability experiment.

Table 2: Rock and fluid properties specified in the CMG model

Properties		Value
Porosity		8-25%
Permeability Range		30-300 md
Temperature		122 °F
Bubble point Pressure		1305 psi
Density	Oil	59.028 lb./ft ³
	Water	62.1456 lb./ft ³
	Gas Gravity	0.70

Water Properties	FVF	1.011
	Compressibility	3.154E-06 1/psi
	Viscosity	0.6135 cp.
Rock Compressibility		1.05E-06 1/psi

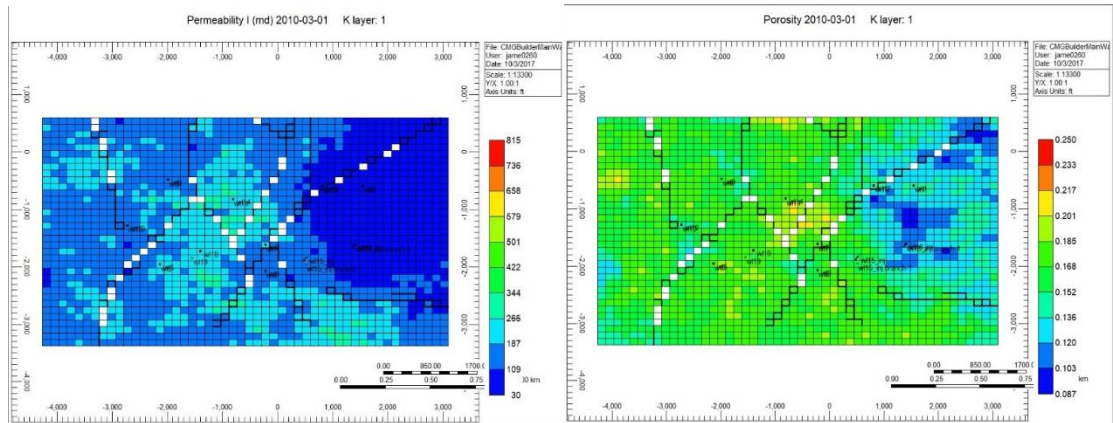


Figure 25: Permeability and porosity maps of the field grid tops. Higher permeability zones were to the center of the simulated field.

Eleven wells were defined in the model, and all were producing wells initially. Two of those wells – Well 15 and 16, were converted to injectors in 2010, while all others were maintained as producing wells. The simulation was run for a period of 20 years.

CHAPTER 5: RESULTS AND DISCUSSION

5.1 Texas Crude and its Deposition Potential

Texas crude showed excellent potential for asphaltene precipitation, especially considering it had a small but significant content of asphaltene that could be easily destabilized. Multiple runs were made to check the asphaltene content of the crude for reproducibility, and the results are shown in **Table 3**.

Table 3: Asphaltene content of Texas crude

Crude		Wt. %	mg/g
Texas Crude	Run 1	1.08	10.78
	Run 2	0.95	9.49
	Run 3	0.62	6.16

Texas crude was determined to have an asphaltene content of about an average asphaltene content of $0.85\% \pm 0.2$, which was similar to the data reported in literature. The test was also run on other crude samples to see how the asphaltene content changes with different samples. A general trend observed was that heavier crudes seemed to have a higher asphaltene content than lighter crudes, but it was in no way an indication that those crudes induced precipitation of asphaltenes. So, the next step was to establish that asphaltene indeed does precipitate out of the crude when mixed with heptane. This was done through the bottle tests, and the results after 24 hours of mixing is shown in **Figure 26**.



Figure 26: Asphaltene precipitation after bottle tests. More precipitation is noted in case of crude mixed with heptane in 1:4 ratio

Based on the observations, it was noticed that Texas crude does indeed cause precipitation of asphaltenes when mixed with heptane. The degree of the precipitation depended on the amount of crude, and a larger precipitation was seen when crude was mixed with heptane in a 4:1 ratio, compared to a 2:1 ratio. Following this, Texas crude was injected into a core sample to determine if this precipitation does indeed happen inside the reservoir. Pressure was monitored continuously, and the data was plotted as shown in **Figure 27**.

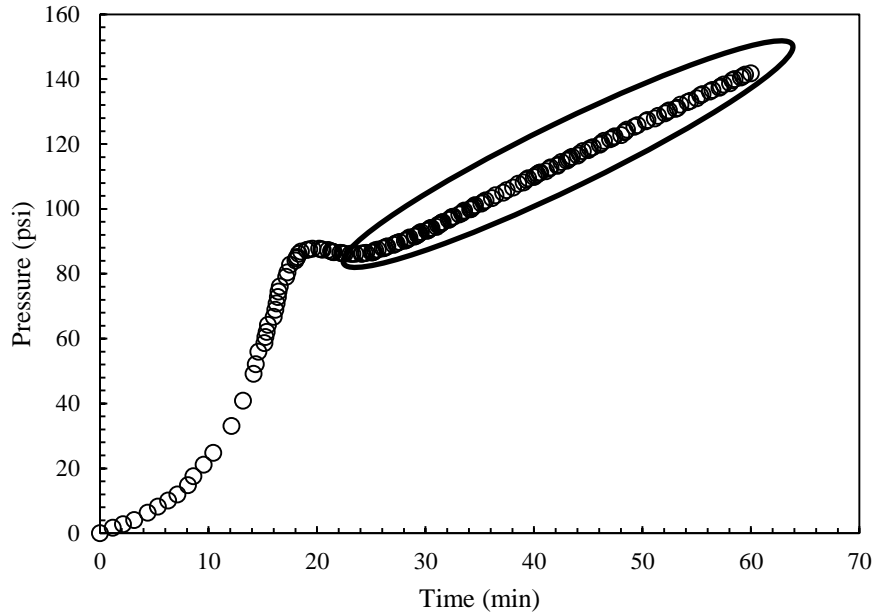


Figure 27: Pressure vs. Time for crude injection. The continuous rise in pressure indicates deposition and clogging of the pore spaces.

Based on the results obtained, it was seen that the pressure increases and then stabilizes for a bit, before starting to rise again. This was indication that there was a blockage of some sort happening in the core, which caused the pressures to rise again, and this result showed that it was due to precipitation of particles from the crude inside the core sample. However, at this stage, it is however difficult to characterize if the blockage was caused by deposition or plugging, or if it is due to asphaltenes, waxes or resins.



Figure 28: Cores after crude injection (left) and after heptane flush (right). The darker tones of the cores indicate the presence of crude residue, even after heptane flush.

5.2 Measuring Rock Properties

Since Grey Berea core samples were used in this study, the properties such as the porosity and permeability were found to be relatively uniform. The porosity of the samples ranged from 18-22%, while the absolute permeability of the samples ranged from 95-160md. The samples were all either 2 or 6 inches in length and all had a diameter of 1 inch. The properties are shown in **Table 4**.

Table 4: Physical properties of cores used in the study

Cores	L (in)	D (in)	W (gm)	ϕ (%)	K (md)	Use
GB-J1-1	1.845	1.00	50.22	21.11	106	Crude Injection Test
GB-J1-3	1.69	1.002	45.87	21.06	-	TOC Test – Crude Injection
GB-J1-4	1.915	0.997	51.81	21.04	-	Crude Injection for Deposition Potential

GB-J1-5	1.740	0.995	47.34	-	-	Spontaneous Imbibition with Brine
GB-J1-6	1.822	0.995	49.33	20.83	-	TOC Test – Control
GB-J2-1	1.958	0.999	51.97	22.49	-	Spontaneous Imbibition- Control
GB-J2-2	1.899	0.996	50.45	22.42	125	Exposed to crude & then Imbibition
GB-J2-3	1.933	0.996	51.53	21.65	140	TOC Test – Saturation
GB-J2-4	1.984	1.000	53.06	22.20	133	Exposed to crude & then Imbibition
GB-J4-2	1.927	1.002	52.39	20.91	116.61	Injected for Deposition Uniformity – Cut Cores 1 inch
GB-J4-3	1.921	0.999	52.4	20.28	102.43	Injected for Deposition Uniformity – Cut Cores 0.5 inch
GB-J6-1	1.909	0.988	50.74	19.14	118.7	Saturated–Uniformity and Pressure
GB-J6-2	1.928	0.986	51	19.25	117.16	Saturated– Uniformity and Pressure
GB-J6-3	1.99	0.985	52.69	19.88	106.7	Saturated–Uniformity and Pressure
GB-J7-1	5.96	0.992	159.7	20.11	135	Relative Perm Clean Sample

GB-J9-2	1.844	0.998	49.90	20.77	118.19	Injected – Uniformity and Pressure
GB-J9-3	1.954	0.996	53.23	19.88	104.86	Pressure Drop Test-Control

Even though the porosities were uniform, there was a noticeable variation in absolute permeabilities of the samples, as seen in **Figure 29**. This was because certain core samples came from a block of Berea, while the other samples were packed individually as separate cores, and so could have been from different blocks of Berea with varying permeabilities.

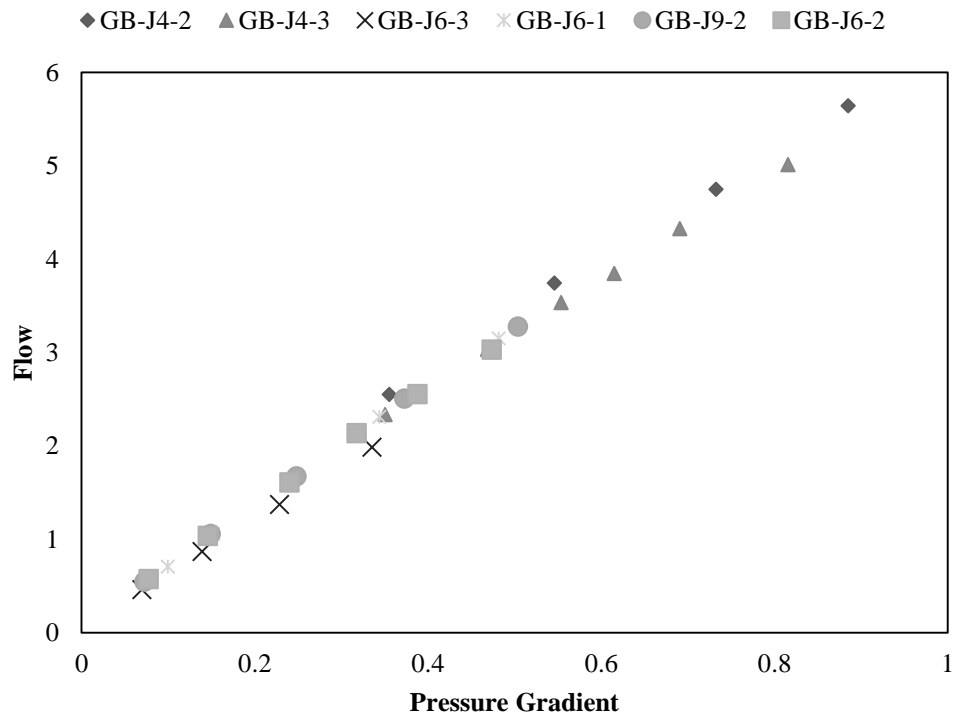


Figure 29: Native permeability's of the core samples ranging from 95-160 md.

In most cases, the absolute permeability calculated by gas Darcy equation at lower flowrates agreed with the absolute permeability calculated using the Forchheimer equation for the non-Darcy flow at higher flowrates, thereby giving more credibility to the permeability values calculated in the lab. The average of the absolute permeabilities calculated using the Gas Darcy equation, and the Forchheimer equation are the results shown in **Table 4** above, and these are the values which were used later to calculate the permeability drop of the core samples due to asphaltene deposition as well as for calculating the relative permeabilities.

5.3 Uniformity of Deposition

The cores which were injected with crude, and those which were vacuum saturated with crude were both checked for determining the uniformity of precipitation by evaluating the density and permeability changes of representative sample sizes, as well as through TOC measurements. The objective was to determine a size of the core sample which is representative of the entire rock, and along which the density and permeability change was uniform. Data from 9 cores was collected for this purpose, of which 3 were used for TOC measurements, and the remaining 6 were used to quantify the density and permeability change.

Of the 6 used to quantify the density and permeability change, 3 were injected with crude, and the remaining 3 were vacuum saturated with crude. 2 of these cores were also cut into smaller pieces to determine representative sample sizes. The list of cores used are noted in **Table 5**. The cores, once they were saturated and aged, were flushed with heptane and dried in an oven.

Table 5: List of cores used for testing uniformity

GB-J4-2	Injected with crude, perm and density measured, cut into halves
GB-J4-3	Injected with crude, perm and density measured, cut into quarters
GB-J6-1	Saturated with Crude, with crude, perm and density measured
GB-J6-2	Saturated with Crude, Co-injected with heptane-crude, perm and density measured
GB-J6-3	Saturated with Crude, with crude, perm and density measured
GB-J9-2	Injected with crude, perm and density measured

Absolute permeability of the cores was measured again, and the data was compared to the initial permeability calculated before any of the experiments. The weights of the core were also measured again, and the densities were recalculated to determine the density change in the core samples. The results are shown in **Table 6** and **Figure 30**.

Table 6: Permeability & density of the cores before and after exposure to crude

Cores	Initial Perm (md)	Final md	% Drop	Initial Wt.	Wt. After	Initial Bulk Density	Final Bulk Density
GB-J4-2	116.61	89.552	23.204	52.385	52.458	2.104	2.107
GB-J4-3	102.43	89.58	12.545	52.4	52.468	2.124	2.127
GB-J6-3	106.7	101.76	4.630	52.69	52.727	2.119	2.12
GB-J6-1	118.7	108.4	8.677	50.74	50.8	2.118	2.12
GB-J6-2	117.16	105.7	9.782	51	51.04	2.114	2.116
GB-J9-2	118.19	98.07	17.023	49.895	49.91	2.113	2.114

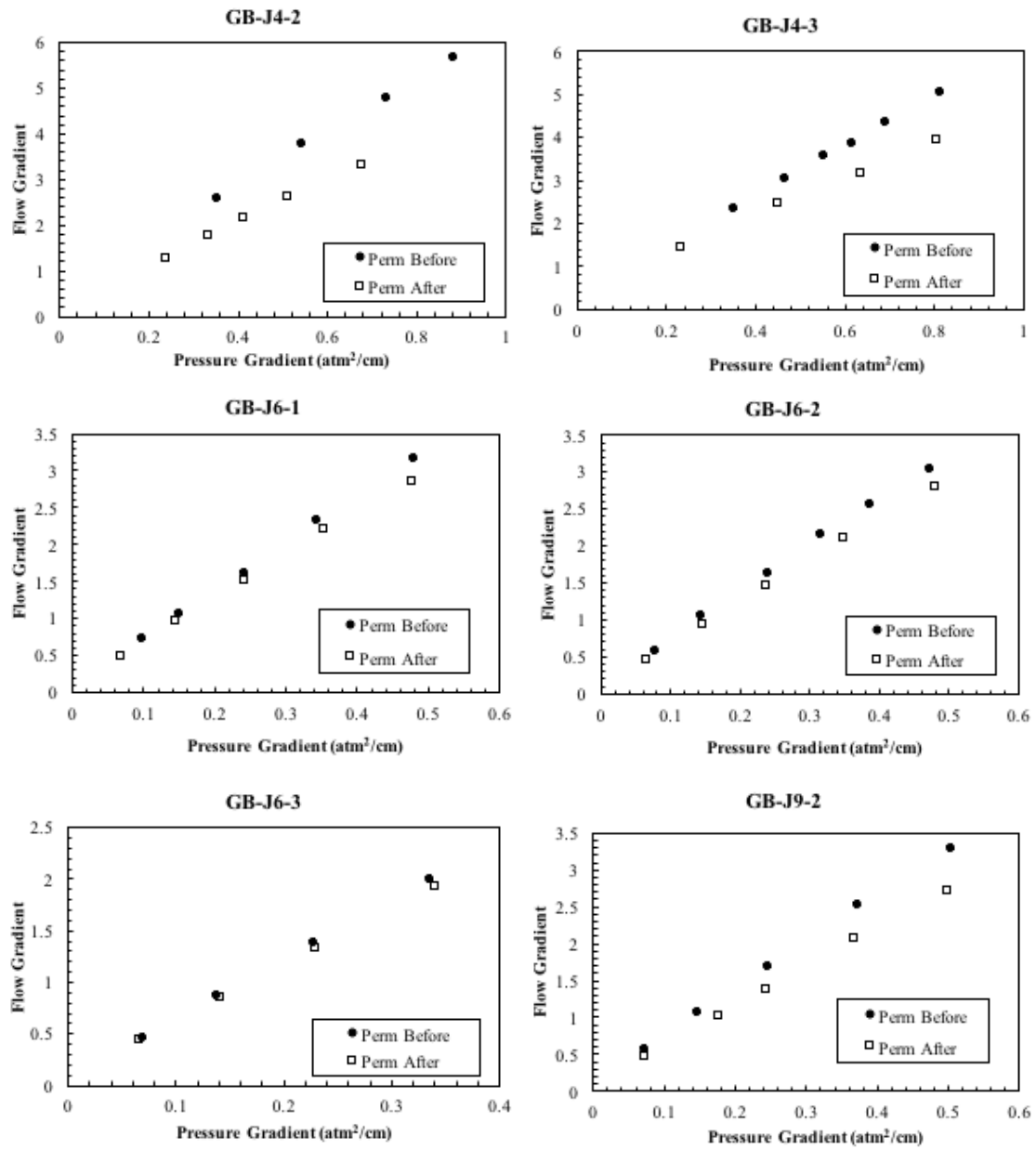


Figure 30: Permeability of the cores before and after the introduction of asphaltenes. The treated cores showed lower permeability compared to the native state.

Based on the results shown above, it was noticed that there was a significant drop in permeability of about 10-20% following injection or saturation with crude. This was also noticed in the density readings of the samples, which increased following the

introduction of crude into the sample. This indicated a precipitation or deposition of crude oil components inside the core. Since the samples were flushed with heptane, it is assumed that the only heavy molecular weight components of crude remaining in the core, and which contributes to this permeability and density change would be asphaltenes. However, this data was not enough to characterize the uniformity of the deposition. For this purpose, the cores were further cut into 1-inch samples, and 0.5-inch samples to see if it was possible to get a representative sample size. The permeability and density measurements are given in **Table 7**.

Table 7: Permeability and density of smaller cut samples

Approx. 1 in length	Perm	Density	Approx. 0.5 in length	Perm	Density
B-J4-2-1	101.26	2.125	GB-J4-3-1-1	40.67	2.126
GB-J4-2-2	80.41	2.121	GB-J4-3-1-2	37.11	2.126
GB-J4-3-1	90.14	2.106	GB-J4-3-2-1	83.20	2.132
GB-J4-3-2	79.67	2.108	GB-J4-3-2-2	54.31	2.125

From the data collected, it was noticed that the bulk density remained consistent at around 2.12 g/cc among the 0.5-inch samples, while the density of the 1-inch samples was still not uniform. Based on this, it was determined that 0.5-inch samples would be a better representative sample size if the experiment is to be scaled up to larger length core sizes. It was also noted that the permeability measurements vary significantly depending on the location of the 1-inch and 0.5-inch samples, ranging from 35-100 md. Since these

cores were injected with crude, this variation in permeability was indication that deposition was not uniform throughout the sample.

Since the data from the permeability and density change experiments were ambiguous regarding uniformity of deposition, Total Organic Content (TOC) measurements were used to further examine this. Of the 3 cores used for TOC measurements, GB-J1-3 was used as a control and was not exposed to any crude; GB-J1-6 was injected with crude and then flushed with heptane; GB-J2-3 was vacuum saturated with crude and then flushed with heptane. The TOC from the inlet, outlet and center of the cores were analyzed, and the data is shown in **Figure 31** below.

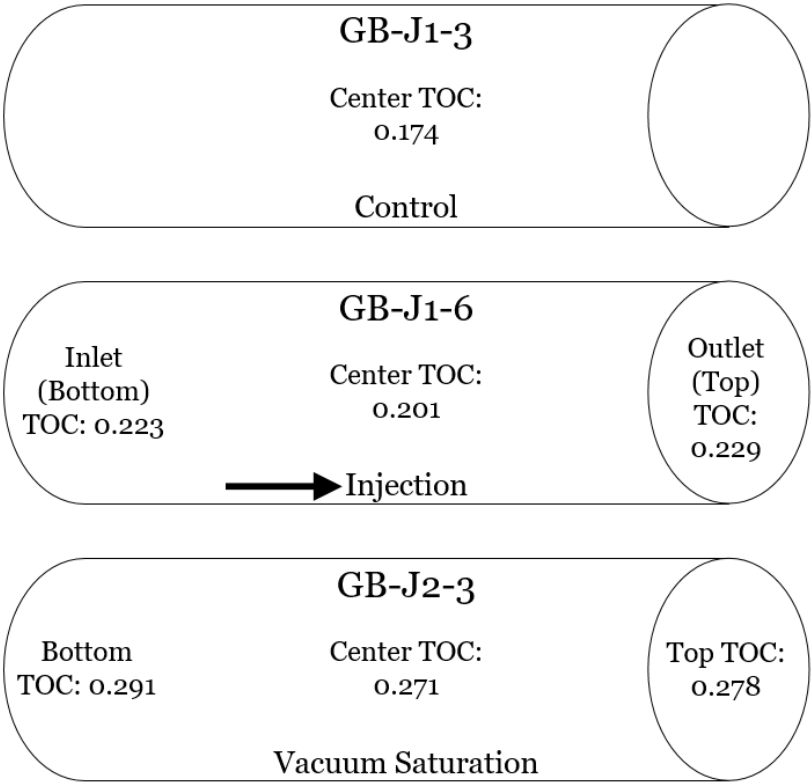


Figure 31: TOC Measurements of the 3 samples at the inlet, outlet and the center. Vacuum saturation showed a better TOC profile throughout the core.

From the TOC measurements, core GB-J1-3 which was used as a control sample had a TOC reading of about 0.174. Cores GB-J2-3, and GB-J1-6 which were subjected to vacuum saturation and injection had significantly higher TOC readings of above 0.2, indicating that organic content was deposited on these Berea core samples. When the TOC content was analyzed at the inlet, outlet and at the center of cores GB-J2-3, and GB-J1-6, it was noticed that core GB-J2-3 which was vacuum saturated had a more uniform TOC profile with readings of 0.291 at the bottom, 0.271 at the center and 0.278 at the top. Core GB-J1-6 which was injected with crude showed the maximum TOC of 0.223 at the inlet, closest to the injection, while the TOC at the center was about 0.201, and 0.229 at the outlet, indicating a non-uniform deposition profile.

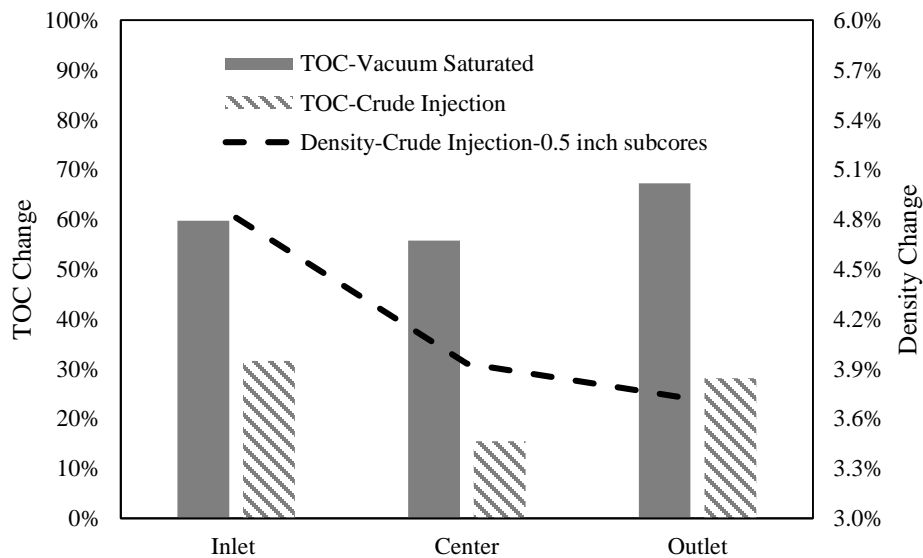


Figure 32: Comparison of TOC with density values for different cores at the inlet, center and the outlet.

When the TOC content from the cores which were injected with crude, and those which were saturated with crude are compared, along with the density change in the samples, a trend was noticed, as shown in **Figure 32**. All the samples tested had a higher

TOC content towards the edges, while lesser towards the center. However, the cores with were vacuum saturated with crude had a higher TOC content, indicating more deposition of asphaltenes, as well as better uniformity in the deposition profile and the density values. Based on all these, even though all the cores used showed a drop in the permeability, and an increase in density when exposed to crude, it was determined that vacuum saturating the Berea cores was a better method to saturate the cores, and create a more uniform deposition profile.

5.4 Core Flood Pressure Drop Tests

Pressure drop tests were conducted on the cores which were saturated with crude to determine any potential wettability alteration, and get an idea on how the relative permeability curves would behave. Five cores were used for this purpose: GB-J9-3, GB-J6-2, GB-J6-3, GB-J9-2 and GB-J6-1. The treatments that were done on the cores are described in **Table 8**.

Table 8: Cores used for pressure drop tests

GB-J9-3	Used as control, no treatment, brine injected, heptane injected
GB-J6-2	Saturated with crude, crude-hep slug injection, hep-crude co-injection, heptane flush, brine injected, heptane injected
GB-J6-3	Saturated with crude, heptane flush, brine injected, heptane injected
GB-J9-2	Clean Rock, Brine injected, crude, heptane flush, brine injected, heptane injected

GB-J6-1	Clean rock, saturated with crude, heptane flush, brine injected, heptane injected (reproducibility)
---------	---

Core GB-J9-3 was used as a control, and was not exposed to any crude during the experiments. Core GB-J9-2 was first injected with brine to establish water wetting phase, and was then saturated with crude. The other cores GB-J6-2, GB-J6-3 and GB-J6-1 were saturated with crude directly and all were aged for a period of 2 weeks to 3 months before the pressure drop tests. After being cleaned, all these cores were then injected with brine, followed by heptane, and pressure was continuously monitored. Brine was used as the initial wetting phase, and heptane the non-wetting phase. The results from the pressure drop across the cores for brine injection and heptane injection are shown in **Figure 33** and **Figure 34**.

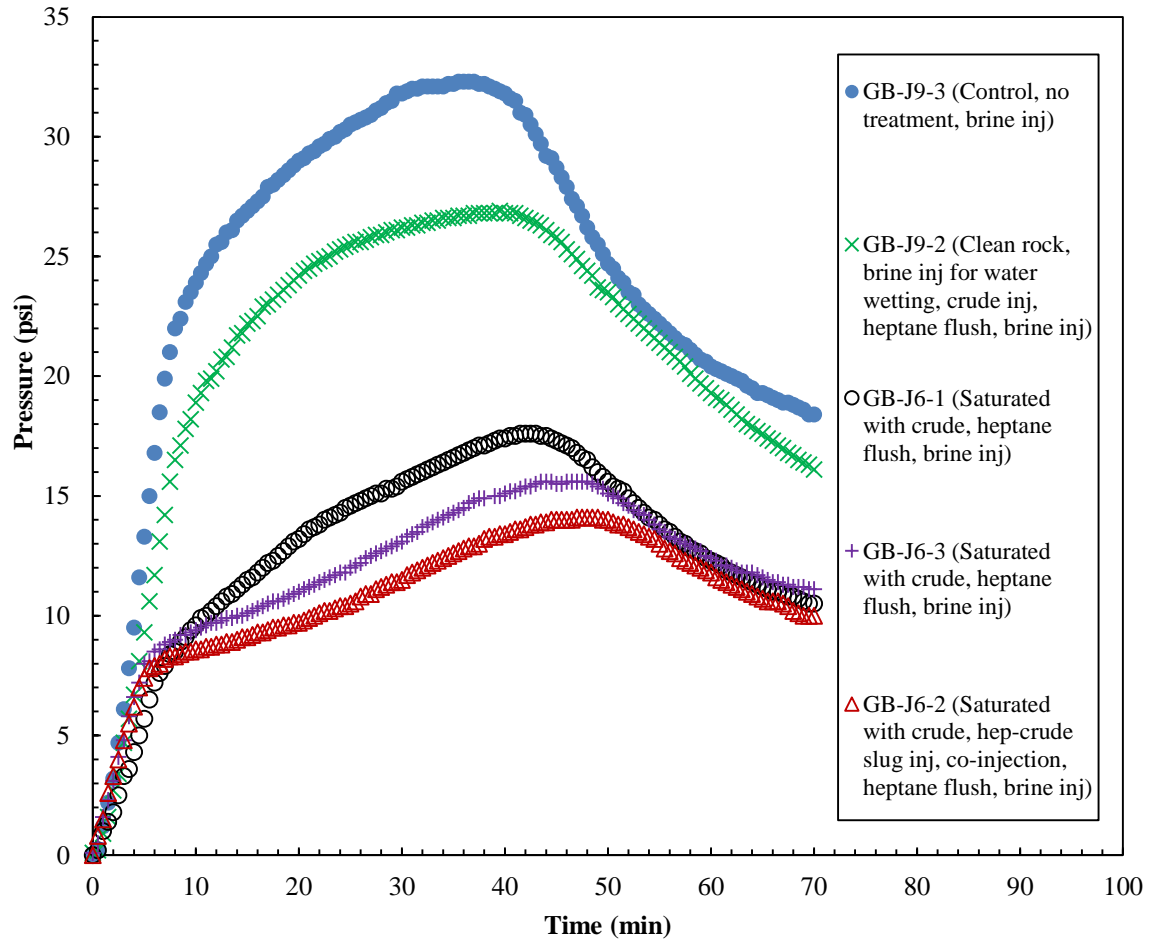


Figure 33: Pressure drops across the cores during brine injection. Higher pressures correspond to a more water wet state.

The pressure tests provide an insight into the wettability of the rock, and possible wettability alteration when exposed to crude or if there is deposition of asphaltenes. Based on the results from the brine injection into the rocks, the largest pressure and the pressure drop was noticed for core GB-J9-3, which was clean and injected with brine first, making it water wet, which corresponds to a larger pressure drop. Even though the pressures didn't rise as high, this was also seen in case of core GB-J9-2, when it was first injected with brine, before being saturated with crude.

Lower pressures and pressure drop was seen in cores GB-J6-1, GB-J6-2 and GB-J6-3 when injected with brine, since these rocks were initially saturated with crude directly and made oil wet before being cleaned with heptane to remove the crude and leaving the asphaltenes behind. Among these three, core GB-J6-2 showed the lowest pressure drop indicating that this core probably was more oil wet than the other two. This could be explained by the fact that GB-J6-2 was also exposed to additional heptane-crude slug injection followed by co-injection, after being saturated and aged, indicating that there was probably more precipitation and deposition of asphaltenes in the core.

In case of core GB-J9-2, after it was saturated with crude and cleaned with heptane, the pressure profile when injected with brine was in between the water wet and oil wet samples. This indicated a mixed wetting status, and was a drop compared to its earlier water wet phase. This was probably because the asphaltene precipitation and deposition inside the core following crude saturation modified its wettability slightly from water wet to oil wet. These results indicated that the asphaltene precipitation inside the cores made it preferentially mixed wet or oil wet, and thus the cores did not react preferentially to brine, even though Berea typically is a water wet sandstone.

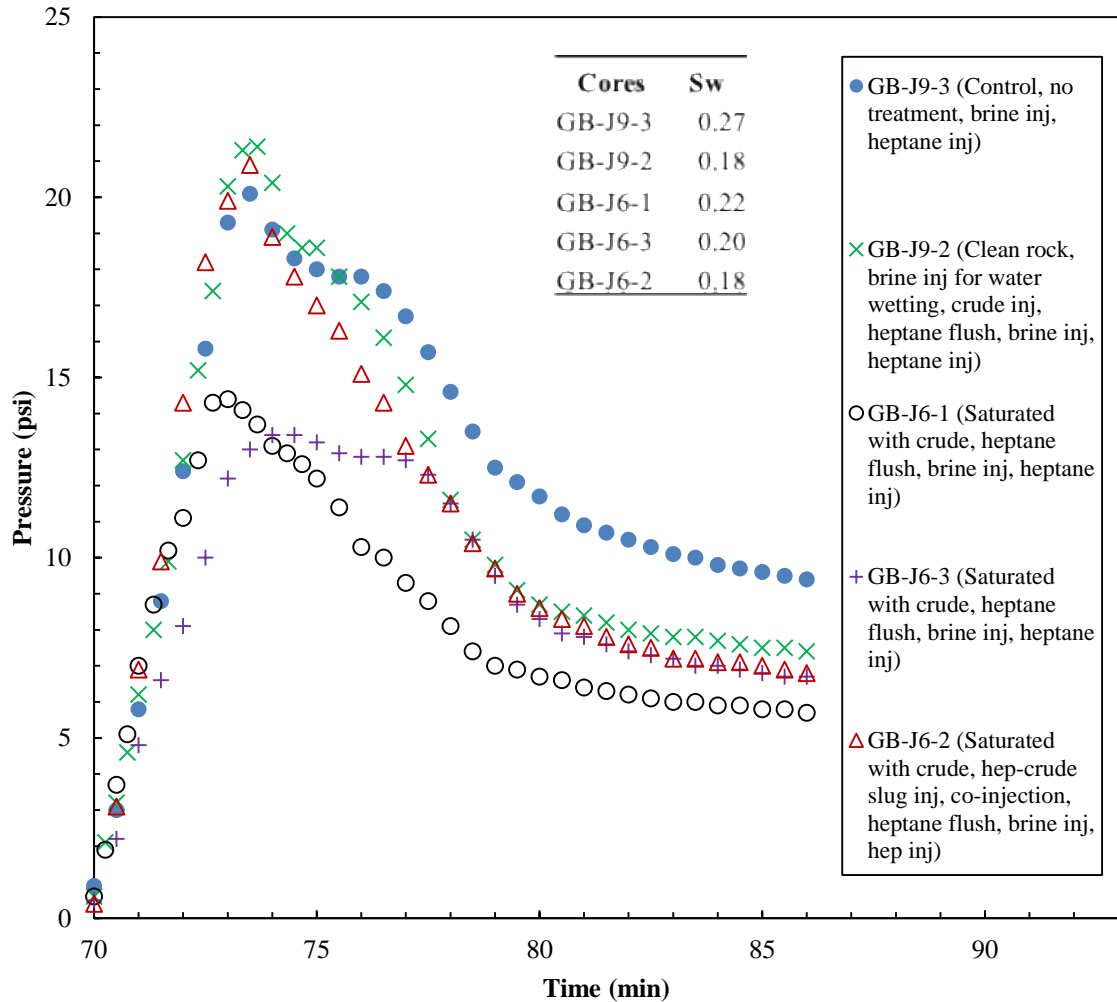


Figure 34: Pressure drop across the cores during heptane injection. Final saturations are also provided to determine the wetting state.

The results were more ambiguous when it came to heptane injection, and the pressure profiles had to be analyzed carefully along with the residual water saturation to understand the wetting phase behavior. Relatively, even though the highest endpoint pressure when heptane is injected is observed in core GB-J9-3, its final water saturation of 0.27 indicated that it is strongly water-wet, and thereby retaining more water. The separation in the pressure profile of GB-J9-3 compared to the other cores is also an indication that it has a different wetting behavior compared to the other cores, which were

either oil or mixed wet. In case of core GB-J9-2, it can be noted from the pressure profile that it is in a mixed wet state compared to the other cores.

When analyzing core GB-J6-2 which was subjected to additional heptane-crude slug injection and co-injection, it can be noted that its pressure profile is lifted compared to cores GB-J6-3 and GB-J6-1. This is expected from an oil wet rock since it would take a higher pressure to displace the oil from the cores. Furthermore, the final water saturation in the core of 0.18 can also be considered as an indicator which further strengthens the earlier inference that it is an oil wet rock. The pressure drops in cores GB-J6-3 and GB-J6-1 which were initially oil wet, is not as pronounced as expected, and this is also reflected in the final water saturation in the core. This could possibly be because the water saturation increased after the brine injection in the first stage, and this brine probably replaced crude oil in certain areas.

5.5 Spontaneous Imbibition Tests

Spontaneous imbibition tests were also conducted on cores exposed to crude oil to further determine the alteration of wettability of the cores. A total of 4 cores were used for this purpose: GB-J2-2 and GB-J2-4 were exposed to crude, while GB-J2-1 was used as a control without being exposed to crude. Imbibition was also done on core GB-J1-5 as a control. The treatments done on the cores are described in **Table 9**: Cores used for spontaneous imbibition, and the treatments done on them..

Table 9: Cores used for spontaneous imbibition, and the treatments done on them.

GB-J2-2	Saturated with crude, aged for 2 weeks, cleaned with heptane and dried. Imbibition done with deionized water. After drying, Imbibition with Heptane
GB-J2-4	Saturated with crude, aged for 2 weeks, cleaned with heptane and dried. Imbibition done with Heptane. After drying, Imbibition with Deionized water
GB-J2-1	Control sample. Imbibition with deionized water. After drying, imbibition with Heptane. Dried and imbibition with deionized water again.
GB-J1-5	Control sample. Imbibition done with 3% NaCl brine.

The recovery of the wetting and non-wetting phases in the core was measured as a function of the weight of the core, and was plotted with time to determine the wettability of the rocks. The buoyancy force was estimated using the volumes, and this was used to estimate the initial weight at time zero. Analysis of this data also helps to determine if there was any change in wettability between the impacted rocks and the control samples. The imbibition results with water is shown below in **Figure 35** and with Heptane in **Figure 36**.

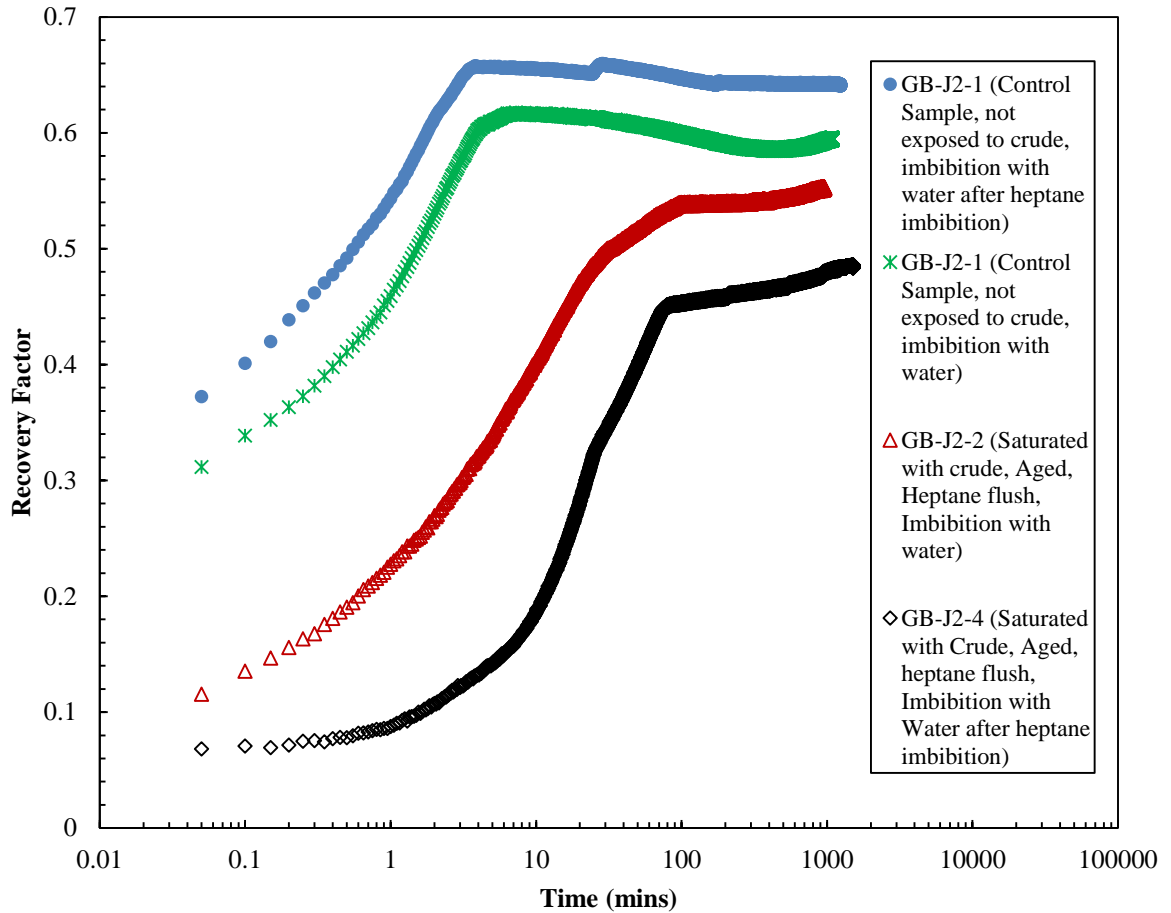


Figure 35: Imbibition results with water. The exposed cores showed a lower imbibition rate and imbibition capacity.

Based on the results, the final water saturations (imbibition capacity) were 55.29% for GB-J2-2, 48.43% for GB-J2-4, 59.54% for GB-J2-1 when measured initially and 64.09% when water imbibition was done again after heptane imbibition. These saturation values are collected after the dry core is immersed in either water, heptane or brine. Based on these results, it can be noted from the graphs that the impacted cores (GB-J2-4 and GB-J2-2) which were saturated with crude and cleaned with n-heptane and dried, had a lower affinity for water during the imbibition test. This could be evident from both the imbibition rate (slope of imbibition curve) and the imbibition capacity. The imbibition

rate for the curve GB-J2-1 which was used as a control, and was not exposed to crude was significantly higher in two cases, when it was exposed to water directly for imbibition, and when it was exposed to water for imbibition after being exposed to heptane. The higher imbibition capacity also indicates that it is more water wet.

From this, it can be noted that the Berea core used as a control achieved a water wet state when it was initially exposed to water for imbibition. It can also be noted that the control core maintained its water wet state even after being exposed to heptane, as seen from the recovery profile of the imbibition by water after heptane imbibition. However, the cores exposed to crude maintained their oil wet state even after being exposed to water imbibition. These results indicated that there was some sort of adsorption or deposition on the core samples which were exposed to crude. Since these cores were flushed with n-heptane in which all crude components except asphaltenes dissolve, it can be certain that there was some asphaltenes left behind in these impacted cores, which made them more oil wet, and reduced their affinity for imbibing water, thereby maintaining a water wet state.

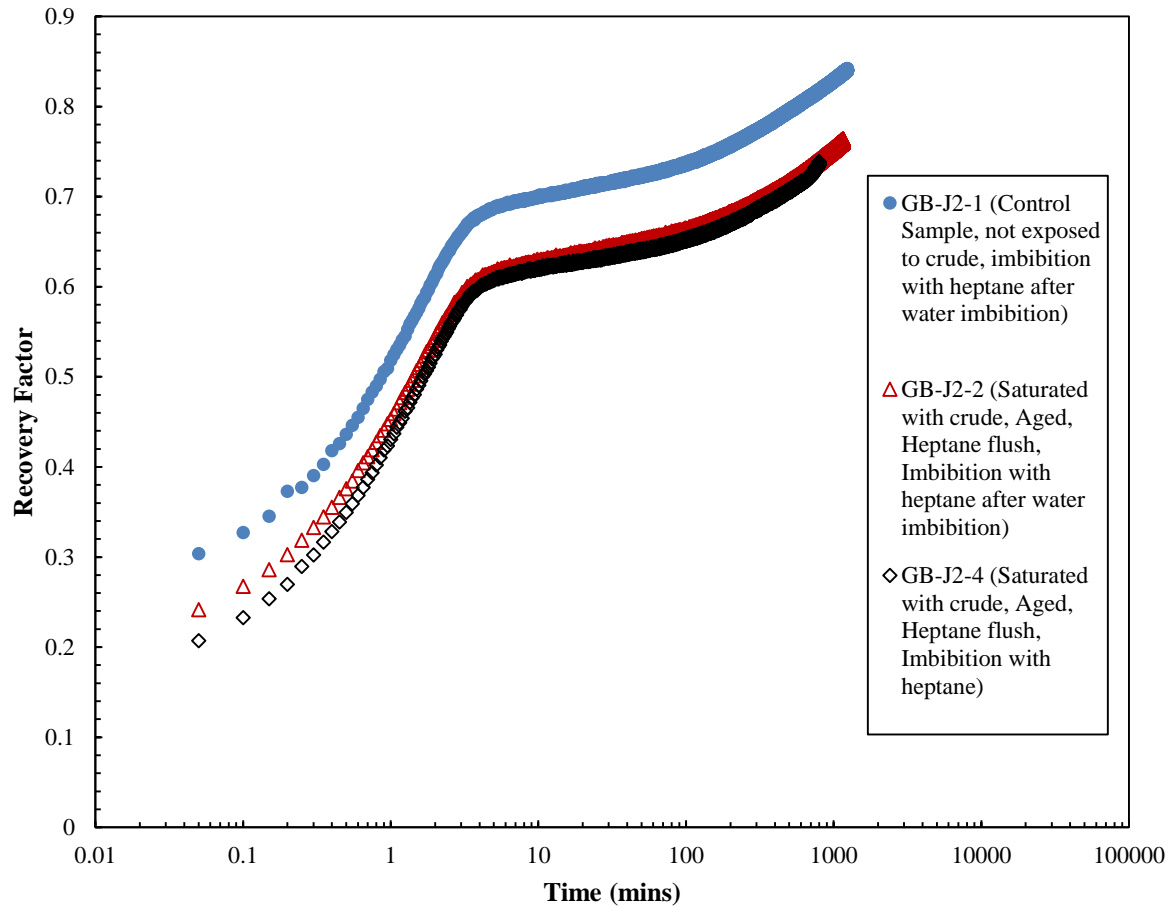


Figure 36: Imbibition results with heptane. Exposed cores show a more neutral wet state or air-heptane imbibition.

During the heptane imbibition tests, the final heptane saturations were 76.26% for GB-J2-2, 73.78% for GB-J2-4 and 84.59% for GB-J2-1 which was used as the control. The results from the heptane imbibition is again a little ambiguous, and should be analyzed based on the order the imbibition tests were done. Since the cores were filled with air, heptane is replacing air in the pore spaces, and so it could be considered as an imbibition run for air-heptane. The imbibition rate for core GB-J2-1 which was used as the control and was subjected to heptane imbibition was higher than both, indicating the clean sample had a higher affinity for oil. Core GB-J2-4, which was exposed to the crude

and was tested with heptane imbibition first, had an imbibition rate and capacity like core GB-J2-2 which was also exposed to crude and tested for heptane imbibition after water imbibition. However, the imbibition rate and capacity when heptane was replacing air in the pores was lower than the clean core, indicating that the deposition of asphaltene somehow altered the wettability to be more neutral wet. This indicated that in an air-heptane system, the clean core is more oil wet, while the asphaltene deposition reduced the oil-wetting state of the exposed cores.

5.6 Relative Permeability Tests

Relative permeability is controlled by the nature of both rock and fluid nature. This fluid nature might be impacted by the salinity content (Mehana & Fahes, 2016). In addition, the rock nature might be impacted by the asphaltene deposition. Therefore, we have conducted a set of relative permeability to quantify this change in wettability which was seen on the cores exposed to crude. The tests were conducted on two 6-inch cores, GB-J7-1 and GB-J10-1. 6 -inch cores were used as longer cores are typically better to quantify relative permeability changes. GB-J7-1 was used as a control, and was not exposed to any crude, while GB-J10-1 was saturated with crude, aged and then cleaned before the relative permeability test. Brine and heptane was used as the two liquids for the relative permeability tests. The treatments done on the cores are described in **Table 10**.

Table 10: Cores used for relative permeability tests.

GB-J7-1	Control Sample. Porosity and Permeability measured. Relative permeability done with brine and heptane
---------	---

GB-J10-1	Porosity and Permeability measured. Core then saturated with crude, aged for 3 months and cleaned with heptane and dried. Relative Permeability endpoints measured with brine and heptane.
----------	--

Absolute permeability and porosity was measured before the experiments began, since this data was required for calculating the relative permeabilities and the saturations at different injection rates. Core GB-J7-1 had a porosity of about 20.11% and permeability of about 135 md. Since GB-J7-1 was used as a control, relative permeability and saturations were measured at several injection rates to develop the relative permeability curves. The data is shown in **Table 11** and **Figure 37**.

Table 11: Relative permeability data points for Brine-Heptane flow.

Sw	Krw	Kro
0.159744	0	0.259199
0.192149	0.019692	0.130954
0.213753	0.020879	0.065768
0.231756	0.025115	0.035161
0.238957	0.033326	0.007488
0.240758	0.036336	0.005676
0.25336	0.04201	0.001811
0.282165	0.048004	0
0.9	0.67	0

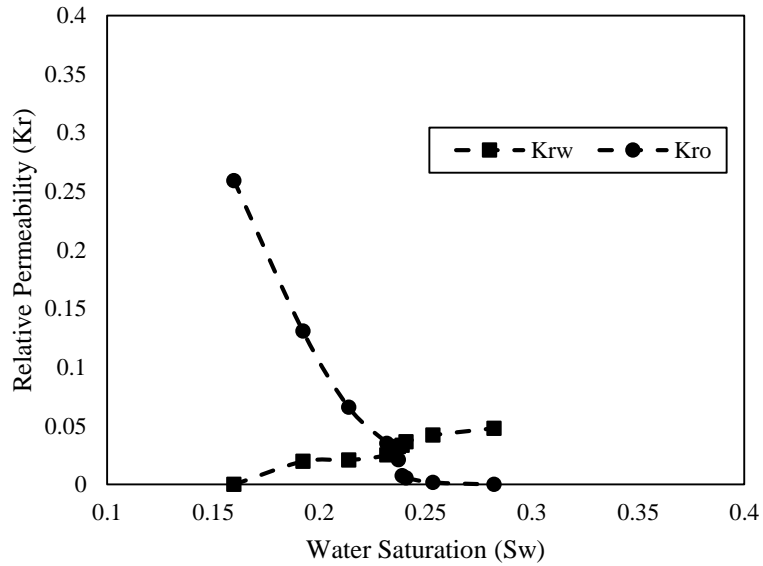


Figure 37: Brine-Heptane relative permeability on a clean sample GB-J7-1

In order to smooth the data, relative permeability tables were generated in CMG using the end points from this experiment. This was used in the CMG simulation model, and is shown in **Figure 38** below.

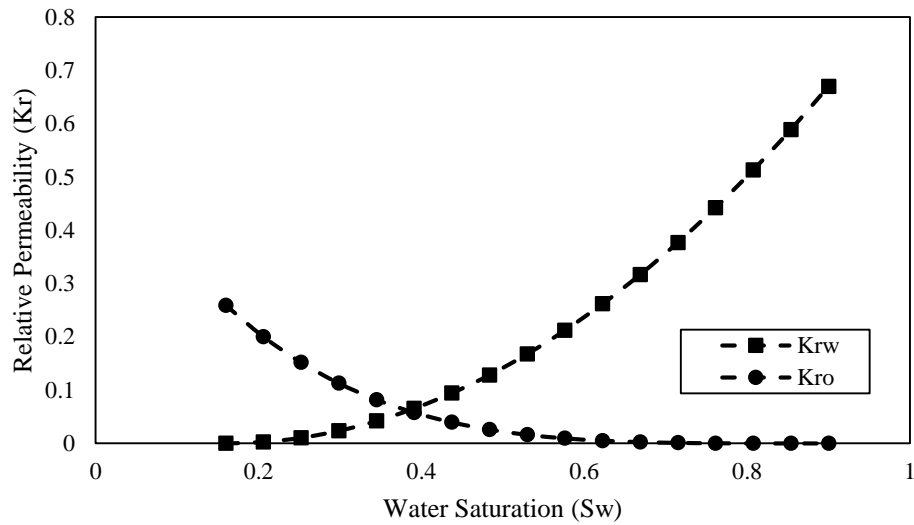


Figure 38: CMG generated curves for Brine-Heptane relative permeability on a clean sample GB-J7-1

For Core GB-J10-1, since the core was exposed to crude and aged, its permeability had to be measured again since a drop in the permeability is expected as per the results of the other experiments done in this study. Based on that data, core GB-J10-1 had a porosity of about 19.86% and reduced permeability of about 98 md. Only the end-point saturations were measured for this core due to time constraints, and additional points were generated using correlations from CMG. The data is shown in **Table 12, Figure 39 and Figure 40.**

Table 12: Brine-Heptane relative permeability endpoints for core exposed to crude

Sw	Krw	Kro
0.405592	0.460585	0
0.135777	0	0.173605

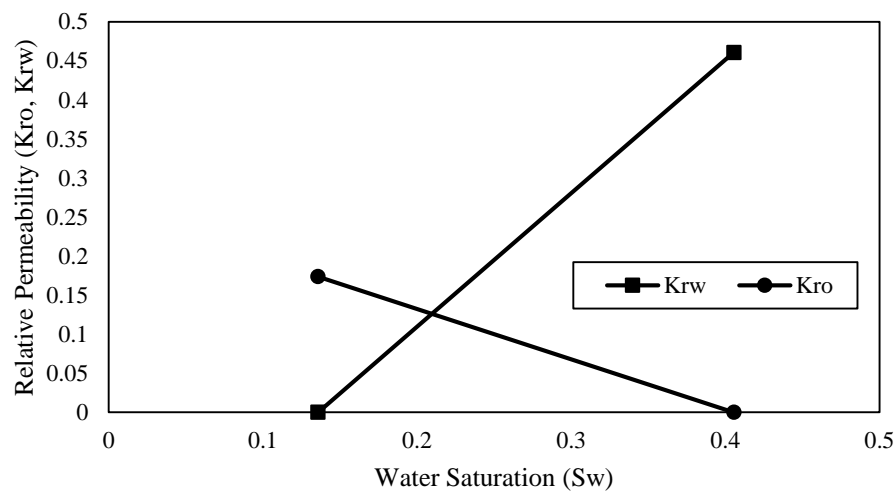


Figure 39: Brine-Heptane relative permeability endpoints for core exposed to crude GB-J10-1

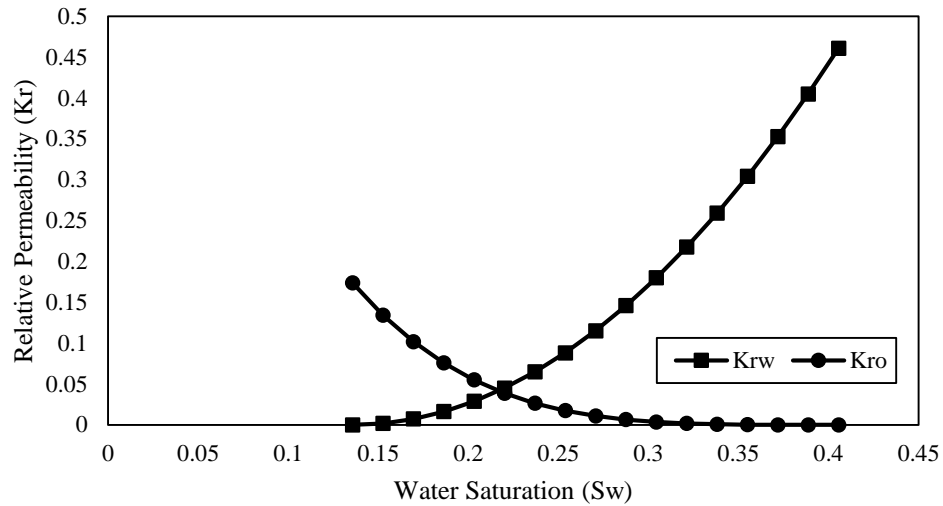


Figure 40: CMG Generated Curves for Brine-Heptane Relative Permeability on a Core Exposed to Crude GB-J10-1

Based on these results, it can be noted that the endpoint saturations have changed significantly between the clean core GB-J7-1, and the impacted core GB-J10-1, as shown **Figure 41**, even though both were Berea cores with comparable porosities and permeabilities. The irreducible water saturation dropped from 16% in the clean core to 13% in the impacted core, while the irreducible oil saturation increased from 10% in the clean core to 59% in the impacted core. The water relative permeability endpoint was also significantly different in case of the clean core indicating that it was a water wet core, while the core which was initially saturated with crude and exposed to asphaltene deposition was more oil wet.

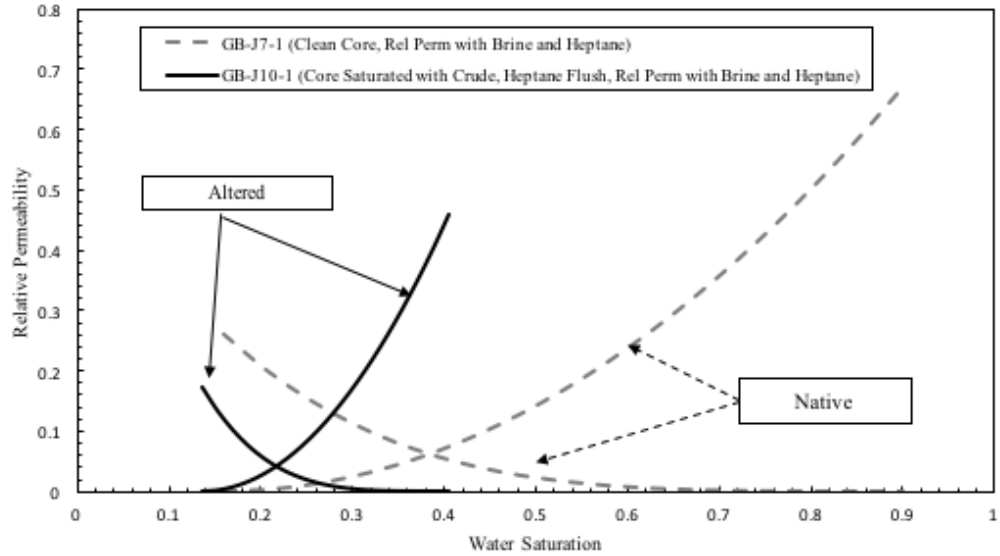


Figure 41: Relative permeability curves for cores GB-J7-1 (clean) and GB-J10-1 (exposed to crude) showing shift in endpoints

5.7 CMG Modeling Results

Using the relative permeability data obtained, the simulation was run, and the results of the water and oil production was compared for the two cases. This helps to determine how the precipitation of asphaltene would affect the overall productivity of the field, with respect to wettability and relative permeability alteration. The simulations were run for a period of 17 years for all 11 wells (including 9 producers and 2 injectors), with a constraint of maximum bottom hole fluid rate. The cumulative oil production, oil rate and water rate are shown in **Figure 42**, **Figure 43** and **Figure 44**.

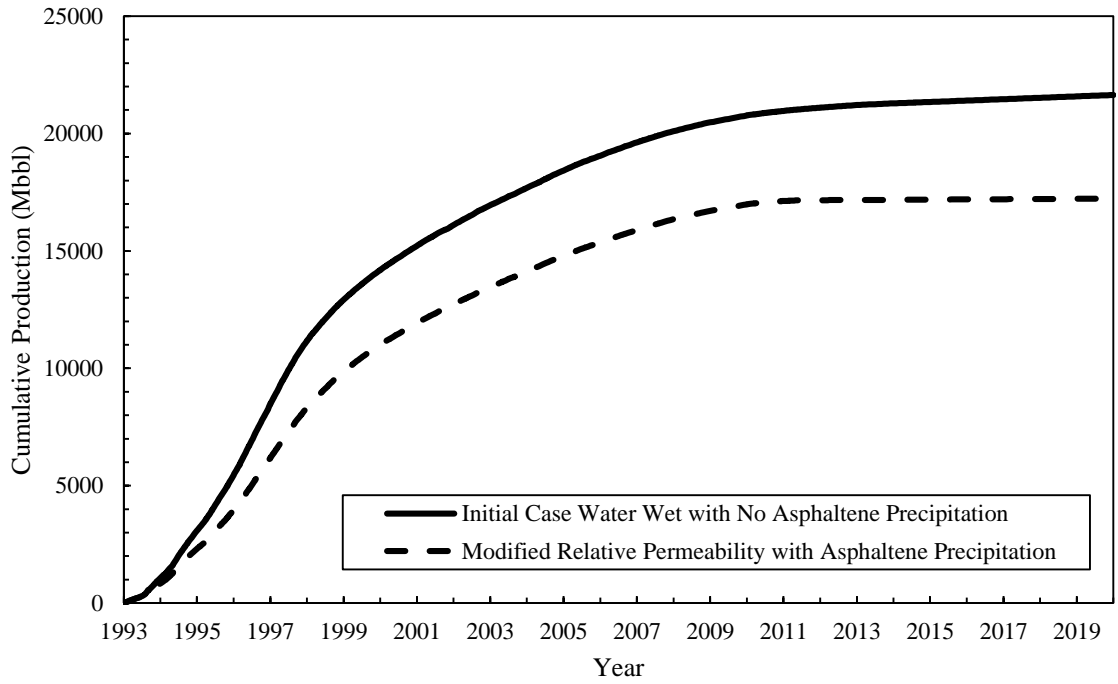


Figure 42: Cumulative Oil Production, Before and After Relative Permeability Modification

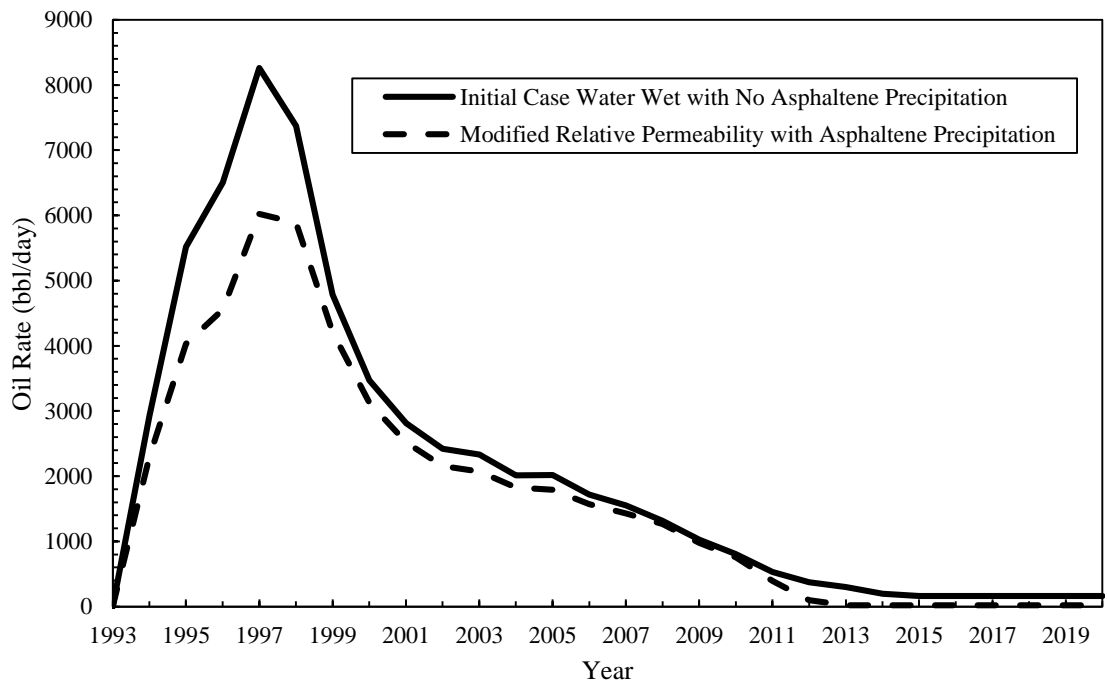


Figure 43: Oil Rate, Before and After Relative Permeability Modification

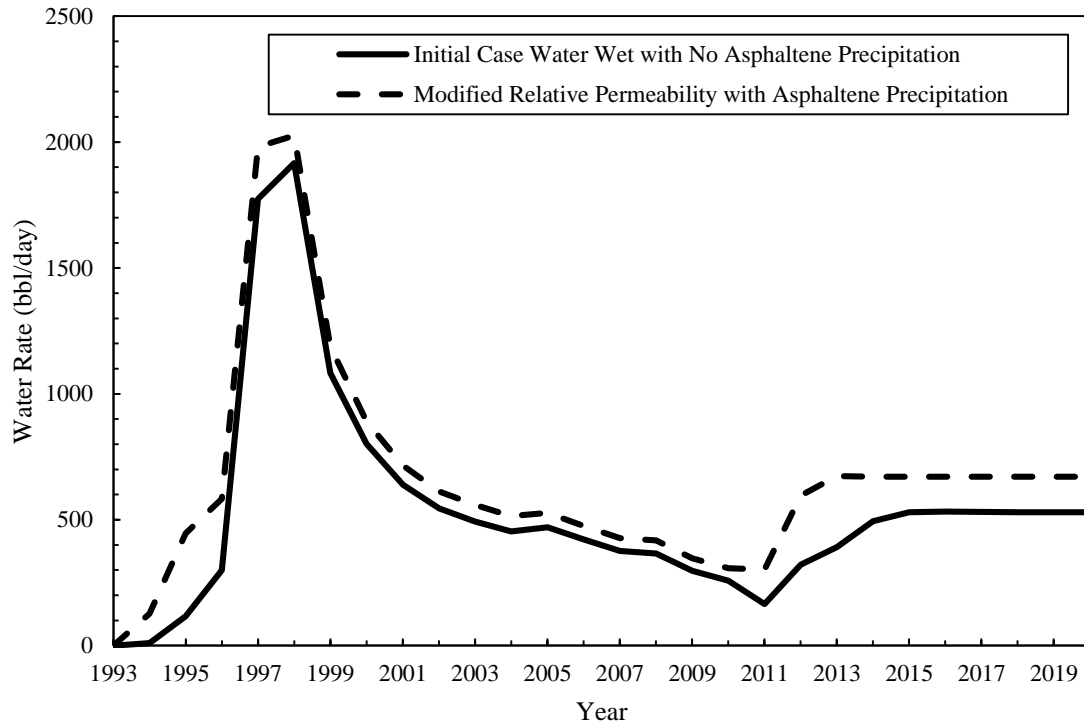
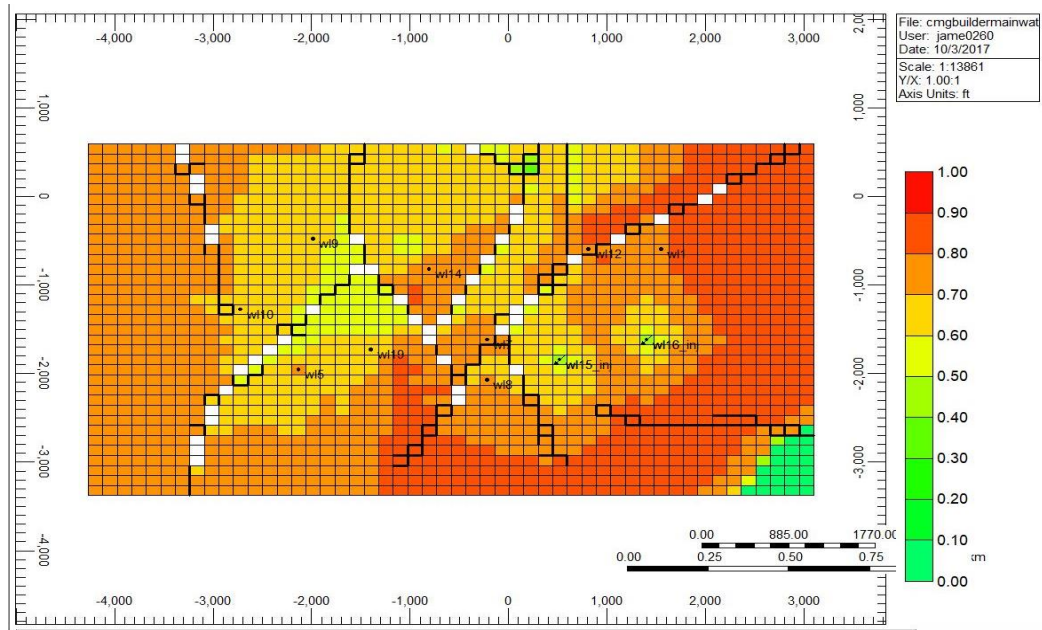


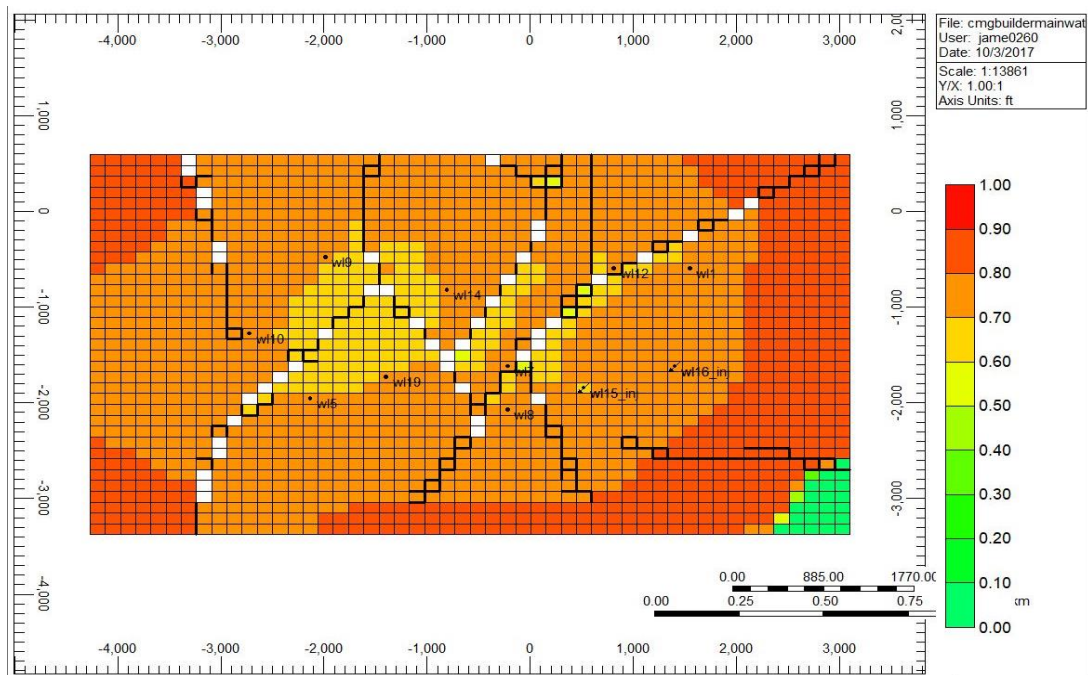
Figure 44: Water Rate, Before and After Relative Permeability Modification

The simulation results were as expected, and it can be clearly noted that a modification of the relative permeability resulted in considerably lower cumulative oil production. The simulation predicted a cumulative production of over 20 million barrels of oil, but actual production would be more around 17 million barrels due to the wettability change in the reservoir. It can also be noted that the actual production rates of oil were lower than the earlier prediction from the unmodified model. The earlier prediction showed a higher production during the initial stages of the simulation compared to the modified model, but both stabilized towards the end of the simulation. The saturations at the end of the simulation runs for both models are shown in **Figure 45** and **Figure 46**.



Native

Figure 45: Native case simulation, with no asphaltene precipitation. Shows higher recovery and lower remaining oil saturation



Modified

Figure 46: Modified case simulation with asphaltene precipitation. Shows lower recovery and higher remaining oil saturation

All this can be attributed to the shift in the saturation and relative permeability endpoints. Additionally, the simulation also under-predicted the oil in place for the two cases with the unmodified model predicting that there was about 258 million barrels of oil in the reservoir, while the modified model predicting there was likely more oil at 265 million barrels, which could be unrecoverable due to the oil/mixed wetting of the reservoir due to asphaltene precipitation. Similarly, the initial model also made an over-prediction of the water in place due to the same reasons.

While this is a simple analysis of what happens on a field scale, the deviations in the model are arguably significant and need to be accounted for. Based on these results, significant over-predictions can be made in reservoir models, if the wettability change and shift in relative permeability due to asphaltene precipitation is not accounted for. This can lead to errors in determining the production data, which has the potential to significantly impact the economics of developing a field.

CHAPTER 6: CONCLUSIONS AND RECOMMENDATIONS

6.1 Conclusions

In this study, the precipitation of asphaltenes on Grey Berea rock samples, and its impact on the rock characteristics were studied. First, a suitable crude was selected, and the crude was tested to ensure that it had asphaltenes, and that it caused a precipitation on the porous media. The uniformity of the deposition was evaluated to determine a suitable method to create a uniform deposit. Wettability changes were then evaluated, before being used in a simulation to determine how the wettability changes would affect the productivity of the field. The following conclusions were made during this study:

- Texas crude which was used in the study had an asphaltene content ranging from 0.6-1.5%, and the crude did induce asphaltene precipitation when injected into Berea core samples.
- Localized deposition was evident in case of injection from a single face, and these results were confirmed through TOC measurements, as well as permeability and density measurements of cut sections from the sample.
- Vacuum saturation of the core with crude produced best results in terms of uniformity of deposition. The results were confirmed through TOC measurements which gave uniform values at the top, bottom and the center of the sample.
- The samples were aged for a period of 2 weeks to 3 months in crude, but the effect of prolonged aging on the samples was not studied.

- Permeability measurements taken after the cores were exposed to crude indicated that there was a drop in absolute permeability of about 10-20%. This result was reproduced in multiple cores.
- A change in the wetting properties was also noticed, with the cores becoming more neutral/intermediate or oil wet, when exposed to crude and the precipitation of asphaltenes.
- The pressure-drop tests conducted on the samples indicated that this wetting change. When samples were injected with brine, a higher pressure drop noticed in case of cores which were not exposed to crude: GB-J9-3 and GB-J9-2, indicating that these cores were water wet. Lower pressure drops were noted for the cores exposed to crude indicating their oil wet state.
- Core GB-J9-2 also indicated a shift in its wetting from water-wet to mixed-wet, after it was saturated with crude.
- Pressure-drop tests with heptane showed comparable results. It was also noted that the core GB-J6-2 which was subject to heptane-oil co-injection had the largest pressure drop when injected with heptane, indicating it was strongly oil wet.
- Imbibition tests conducted on the samples reinforced the wettability change in the cores, with cores which were exposed to crude showing a more pronounced oil-wet state.
- Relative permeability end points were calculated during two-phase flow, and correlations in CMG was used to generate the relative permeability curves. There

was a shift in the end-point saturations with the exposed cores showing a lower irreducible water saturation.

- Modeling of this wettability change on CMG indicated that this wettability change, if not accounted for, will lead to over-estimation of the recoverable reserves in place. There was also a drop cumulative production of about 3 million barrels due to the shift in the relative permeability curves.

6.2 Recommendations

Further studies in this area could tackle the following:

- Repeat the study using different crudes with different asphaltene contents.
- Quantifying the asphaltene precipitation tendency using acid number (TAN/TBN) measurements.
- Study the effect of different aging periods, and temperature on the wetting alteration.
- Conduct a molecular simulation to better understand the intermolecular forces associated with asphaltene deposition and adsorption (Mehana, Fahes, & Liangliang, 2017).

References

- Akbarzadeh, K., Hammami, A., Kharrat, A., Zhang, D., Allenson, S., Creek, J., . . . Solbakken, T. (2007). *Asphaltenes—Problematic but Rich in Potential*. Oilfield Review.
- Amroun, H., & Tiab, D. (2001). Alteration of Reservoir Wettability Due to Asphaltene Deposition in Rhourd-Nouss Sud Est Field, Algeria. *SPE Rocky Mountain Petroleum Technology Conference*. Keystone, Colorado: Society of Petroleum Engineers.
- ASTM International. (2005). *Standard Test Method for Determination of Asphaltenes (Heptane Insolubles) in Crude Petroleum and Petroleum Products*. ASTM International.
- Blunt, M. J., Al-Jadi, M., Al-Qattan, A., Al-Kanderi, J. M., Gharbi, O., Badamchizadeh, A., . . . Skoreyko, F. A. (2012). Evaluation of the Effect of Asphaltene Deposition in the Reservoir for the Development of the Magwa Marrat Reservoir. *SPE Kuwait International Petroleum Conference and Exhibition*. Kuwait City: Society of Petroleum Engineers.
- Crain, E. R. (2006). *Crain's Petrophysical Handbook*.
- Dahaghi, A. K., Gholami, V., Moghadasi, J., & Abdi, R. (2008). Formation Damage through Asphaltene Precipitation Resulting from CO₂ gas injection in Iranian Carbonate Reservoirs. *SPE Production and Operations*, 210-214.
- De La Cruz, J. L., Argüelles-Vivas, F. J., Matías-Pérez, V., Durán-Valencia, C. A., & López-Ramírez, S. (2009). Asphaltene-Induced Precipitation and Deposition During Pressure Depletion on a Porous Medium: An Experimental Investigation and Modeling Approach. *Energy & Fuels*, 5611–5625.
- Dehgani, M., Ali, S., Vafaie-Sefti, M., Mirzayi, B., & Fasih, M. (2007). Experimental Investigation on Asphaltene Deposition in Porous Media During Miscible Gas Injection. *Iran Journal of Chemistry and Chemical Engineering*, 39-48.
- Eskin, D., Mohammadzadeh, O., Akbarzadeh, K., Taylor, S. D., & Ratulowski, J. (2016). Reservoir Impairment by Asphaltenes: A Critical Review. *The Canadian Journal of Chemical Engineering*, 94, 1202-1217.

- Goual, L., & Firoozabadi, A. (2004). Effect of Resins and DBSA on Asphaltene Precipitation from Petroleum Fluids. *AIChE Journal*, 50(2), 470-479.
doi:10.1002/aic.10041
- Hasanvand, M. Z., Ahmadi, M. A., & Behbahani, R. M. (2015). Solving asphaltene precipitation issue in vertical wells via redesigning of production facilities. *Petroleum*, 139-145.
- Haskett, C. E., Tartera, M., & Polumbus, E. A. (1984). A Practical Solution to the Problem of Asphaltene Deposits- Hassi Messaoud Field, Algeria. *SPE 39th Annual Fall Meeting* (pp. 387-391). Houston, Texas: SPE Production Operations.
- Hayashi, Y., & Okabe, H. (2010). Experimental Investigation of Asphaltene Induced Permeability Reduction. *SPE EOR Conference at Oil & Gas West Asia*. Muscat: Society of Petroleum Engineers.
- Hematfar, V., Maini, B. B., & Chen, Z. (2013). Experimental Investigation of the Impact of Asphaltene Adsorption on Two Phase Flow in Porous Media. *SPE European Formation Damage Conference and Exhibition*. Noordwijk, Netherlands.
- Honarpour, M., & Mahmood, S. M. (1988). Relative-Permeability Measurements: An Overview. *SPE Journal of Petroleum Technology*, 963-966.
- Hopkins, P. A., Walrond, K., Strand, S., Puntervold, T., Austad, T., & Wakwaya, A. (2016). Adsorption of Acidic Crude Oil Components onto Outcrop Chalk at Different Wetting Conditions during Both Dynamic Adsorption and Aging Processes. *Energy and Fuel*, 30, 7229-7235.
- Huang, H., & Ayoub, J. A. (2008). Applicability of the Forchheimer Equation for Non-Darcy Flow in Porous Media. *SPE Journal*, 13(01), 112-122.
doi:<https://doi.org/10.2118/102715-PA>
- Jia, D., Buckley, J. S., & Morrow, N. R. (1991). Control of Core Wettability with Crude Oil. *SPE International Symposium on Oilfield Chemistry*, (pp. 401-409). Anaheim, California.
- Ju, B., Qiu, X., Qin, J., Chen, X., & Fan, T. (2010). Asphaltene Deposition and Its Effects on Production Performances in the Development of Oil Field by CO₂ Flooding: A Numerical Simulation Assessment. *SPE EUROPEC/EAGE Annual Conference and Exhibition*. Barcelona.

- Kazemzadeh, Y., Malayeri, M. R., Riazi, M., & Parsaei, R. (2014). Impact of Fe₃O₄ nanoparticles on asphaltene precipitation during CO₂ Injection. *Journal of Natural Gas Science and Engineering*, 22, 227-234.
- Khanifar, A., Onur, M., & Darman, N. (2014). New Experimental Correlations to predict water-oil relative permeability curves affected from asphaltene deposition. *Offshore Technology Conference-Asia*. Kuala Lumpur: Offshore Technology Conference.
- Kocabas, I. (2003). Characterization of Asphaltene Precipitation Effect on Reducing Carbonate Rock Permeability. *Middle East Oil Show*. Manama, Bahrain: Society of Petroleum Engineers.
- Kord, S., Mohammadzadeh, O., Miri, R., & Soulgani, B. S. (2013). Further investigation into the mechanisms of asphaltene deposition and permeability impairment in porous media using a modified analytical model. *Fuel*, 259-268.
- Leontaritis, K. J., & Mansoori, G. A. (1988). Asphaltene Deposition: A Survey of Field Experiences and Research Approaches. *Journal of Petroleum Science and Engineering*, 1(3), 229-239.
- Mehana, M. Z., Fahes, M., & Liangliang, H. (2017). System Density of Oil-Gas Mixtures: Insights from Molecular Simulations. *SPE Annual Technical Conference and Exhibition*. San Antonio, Texas, USA: Society of Petroleum Engineers.
- Mehana, M., & Fahes, M. (2016). The Impact of the Geochemical Coupling on the Fate of Fracturing Fluid, Reservoir Characteristics and Early Well Performance in Shale Reservoirs. . *SPE Kingdom of Saudi Arabia Annual Technical Symposium and Exhibition*. Dammam, Saudi Arabia: Society of Petroleum Engineers.
- Mehana, M., Al Salman , M., & Fahes, M. (2017). The Impact of Salinity on Water Dynamics, Hydrocarbon Recovery and Formation Softening in Shale: Experimental Study. *SPE Kingdom of Saudi Arabia Annual Technical Symposium and Exhibition*. Dammam, Saudi Arabia: Society of Petroleum Engineers.
- Minssieux, L. (1997). Core damage from crude asphaltene deposition. *SPE Oilfield Chemistry Symposium*. Houston, Texas.
- Minssieux, L., Nabzar, L., Chauveteau, G., Longeron, D., & Bensalem, R. (1998). Permeability Damage due to Asphaltene deposition: Experimental and Modeling Aspects. *REVUE DE L'INSTITUT FRANÇAIS DU PÉTROLE*, 53, 313-327.

- Mirzayi, B., Vafaie-Sefti, M., Mousavi-Dehghani, S. A., Fasih, M., & Mansoori, G. A. (2008). The Effects of Asphaltene Deposition on Unconsolidated Porous Media Properties during Miscible Natural Gas Flooding. *Petroleum Science and Technology*, 231-243.
- Mukhametshina, A., Kar, T., & Hascakir, B. (2015). Asphaltene Precipitation during Bitumen Extraction with Expanding Solvent Steam Assisted Gravity Drainage: Effects on Pore Scale Displacement. *SPE Journal*, 21, 380-392.
- Nasri, Z., & Dabir, B. (2009). Effect of Asphaltene Deposition on Oil Reservoir Characteristics Including Two Phase flow. *Journal of Japan Petroleum Institute*, 52, 1-9.
- Rezaian, A., Kordestany, A., Jamialahmadi, M., Moghadasi, J., Khoshdaregi, M. Y., Alipanah, M., & Sefat, M. H. (2010). Experimental and Theoretical Studies of Flocculated Asphaltene Deposition From Oil in Porous Media. *Trinidad and Tobago Energy Resources Conference*. Port of Spain: Society of Petroleum Engineers.
- Rogel, E., Miao, T., Vien, J., & Roe, M. (2015). Comparing Asphaltenes: Deposit vs. Crude. *Fuel*, 155-160.
- Shabib-Asl, A., Ayoub, M. A., Saaïd, I. M., & Valentim, P. P. (2015). Experimental Investigation into Effects of Crude Oil Acid and Base Number on Wettability Alteration. *Journal of Japan Petroleum Institute*, 58, 228-236.
- Shedid, S. A. (2001). Influences of Asphaltene Precipitation on Capillary Pressure and Pore Size Distribution of Carbonate Reservoirs. *Petroleum Science and Technology*, 19, 503-519.
- Shedid, S. A., & Abbas, E. A. (2005). An Experimental Approach of the Reversibility of Asphaltene Deposition under Dynamic Flow Conditions. *SPE Middle East Oil and Gas Show and Conference*. Manama, Bahrain: Society of Petroleum Engineers.
- Sim, S. S., Okatsu, K., Takabayashi, K., & Fisher, D. B. (2005). Asphaltene-Induced Formation Damage: Effect of Asphaltene Particle Size and Core Permeability. *SPE Annual Technical Conference and Exhibition*. Dallas, Texas: Society of Petroleum Engineers.
- Stankiewicz. (2009). Origin and Behavior of Oil Asphaltenes - Integration of Disciplines. *SPE Distinguished Lecture Series*.

- Vargas, F. M., Garcia-Bermudes, M., Boggara, M., Punnapala, S., Abutaqiya, M., Mathew, N., . . . Al-Asafen, H. (2014). On the Development of an Enhanced Method to Predict Asphaltene Precipitation. *Offshore Technology Conference*. Houston, Texas.
- Wolcott, J. M., Groves, F., & Lee, H. G. (1996). The Influence of Crude-Oil Composition on Mineral Adsorption and Wettability Alteration. *SPE International Symposium on Oilfield Chemistry*. New Orleans, Louisiana.
- Zanganeh, P., Ayatollahi, S., Alamdari, A., Zolghadr, A., Dashti, H., & Kord, S. (2011). Asphaltene Deposition during CO₂ Injection and Pressure Depletion: A Visual Study. *Energy & Fuel*, 1412-1419.
- Zekri, A. Y., Shedid, S. A., & Almehaieb, R. A. (2009). Sulfur and Asphaltene Deposition During CO₂ Flooding of Carbonate Reservoirs. *SPE Middle East Oil and Gas Show and Conference*. Manama, Bahrain: Society of Petroleum Engineers.
- Zendehboudi, S., Shafiei, A., Bahadori, A., James, L. A., Elkamel, A., & Lohi, A. (2014). Asphaltene precipitation and deposition in oil reservoirs – Technical aspects, experimental and hybrid neural network predictive tools. *Chemical Engineering Research and Design*, 92(5), 857-875.
- Zhou, Y. (2011). *A Study of the Potential of Asphaltene Precipitation due to Gas Injection in a UAE Carbonate Reservoir*. Abu Dhabi: The Petroleum Institute.